Infection and Drug Resistance

Dovepress
open access to scientific and medical research

Open Access Full Text Article

ORIGINAL RESEARCH

N-Acetyl-Cysteine Increases Activity of Peanut-Shaped Gold Nanoparticles Against Biofilms Formed by Clinical Strains of *Pseudomonas aeruginosa* Isolated from Sputum of Cystic Fibrosis Patients

Ewelina Piktel[1], Urszula Wnorowska[1], Joanna Depciuch[2], Dawid Łysik[3], Mateusz Cieśluk[1], Krzysztof Fiedoruk[1], Joanna Mystkowska[3], Magdalena Parlińska-Wojtan[2], Paul A Janmey[4], Robert Bucki[1]

[1]Department of Medical Microbiology and Nanobiomedical Engineering, Medical University of Białystok, Białystok, 15-222, Poland; [2]Institute of Nuclear Physic, Polish Academy of Sciences, Krakow, PL-31342, Poland; [3]Institute of Biomedical Engineering, Bialystok University of Technology, Bialystok, 15-351, Poland; [4]Department of Physiology and Institute for Medicine and Engineering, University of Pennsylvania, Philadelphia, PA, 19102, USA

Correspondence: Robert Bucki, Department of Medical Microbiology and Nanobiomedical Engineering, Medical University of Bialystok, Mickiewicza 2C, Bialystok, 15-222, Poland, Tel + 48 85 748 5793, Email buckirobert@gmail.com

Infection and Drug Resistance downloaded from https://www.dovepress.com/
For personal use only.

Background: Extracellular polymeric substances (EPS) produced by bacteria, as they form a biofilm, determine the stability and viscoelastic properties of biofilms and prevent antibiotics from penetrating this multicellular structure. To date, studies demonstrated that an appropriate optimization of the chemistry and morphology of nanotherapeutics might provide a favorable approach to control their interaction with EPS and/or diffusion within the biofilm matrix. Targeting the biofilms' EPS, which in certain conditions can adopt liquid crystal structure, was demonstrated to improve the anti-biofilm activity of antibiotics and nanoparticles. A similar effect is achievable by interfering EPS' production by mucoactive agents, such as N-acetyl-cysteine (NAC). In our previous study, we demonstrated the nanogram efficiency of non-spherical gold nanoparticles, which due to their physicochemical features, particularly morphology, were noted to be superior in antimicrobial activity compared to their spherical-shaped counterparts.

Methods: To explore the importance of EPS matrix modulation in achieving a suitable efficiency of peanut-shaped gold nanoparticles (AuP NPs) against biofilms produced by *Pseudomonas aeruginosa* strains isolated from cystic fibrosis patients, fluorescence microscopy, as well as resazurin staining were employed. Rheological parameters of AuP NPs-treated biofilms were investigated by rotational and creep-recovery tests using a rheometer in a plate-plate arrangement.

Results: We demonstrated that tested nanoparticles significantly inhibit the growth of mono- and mixed-species biofilms, particularly when combined with NAC. Notably, gold nanopeanuts were shown to decrease the viscosity and increase the creep compliance of *Pseudomonas* biofilm, similarly to EPS-targeting NAC. Synergistic activity of AuP NPs with tobramycin was also observed, and the AuP NPs were able to eradicate bacteria within biofilms formed by tobramycin-resistant isolates.

Conclusion: We propose that peanut-shaped gold nanoparticles should be considered as a potent therapeutic agent against *Pseudomonas* biofilms.

Keywords: gold nanoparticles, non-spherical nanoparticles, N-acetyl-cysteine, bacteria biofilm, cystic fibrosis, *Pseudomonas aeruginosa*

Introduction

Despite the clinical introduction of a spectrum of therapeutics with anti-bacterial and/or anti-inflammatory activities along with agents facilitating clearance of airways from thick and dehydrated sputum, the mortality rate of patients suffering from cystic fibrosis (CF) is still alarmingly high.[1] Chronic inflammation and persistent *Pseudomonas aeruginosa* colonization are recognized as the major causes of lung tissue damage, lung transplantation, and mortality in CF subjects.[2] Regardless of the

Received: 12 November 2021
Accepted: 9 February 2022
Published: 5 March 2022

© 2022 Piktel et al. This work is published and licensed by Dove Medical Press Limited. The full terms of this license are available at https://www.dovepress.com/terms.php and incorporate the Creative Commons Attribution – Non Commercial (unported, v3.0) License (http://creativecommons.org/licenses/by-nc/3.0/). By accessing the work you hereby accept the Terms. Non-commercial uses of the work are permitted without any further permission from Dove Medical Press Limited, provided the work is properly attributed. For permission for commercial use of this work, please see paragraphs 4.2 and 5 of our Terms (https://www.dovepress.com/terms.php).

Graphical Abstract

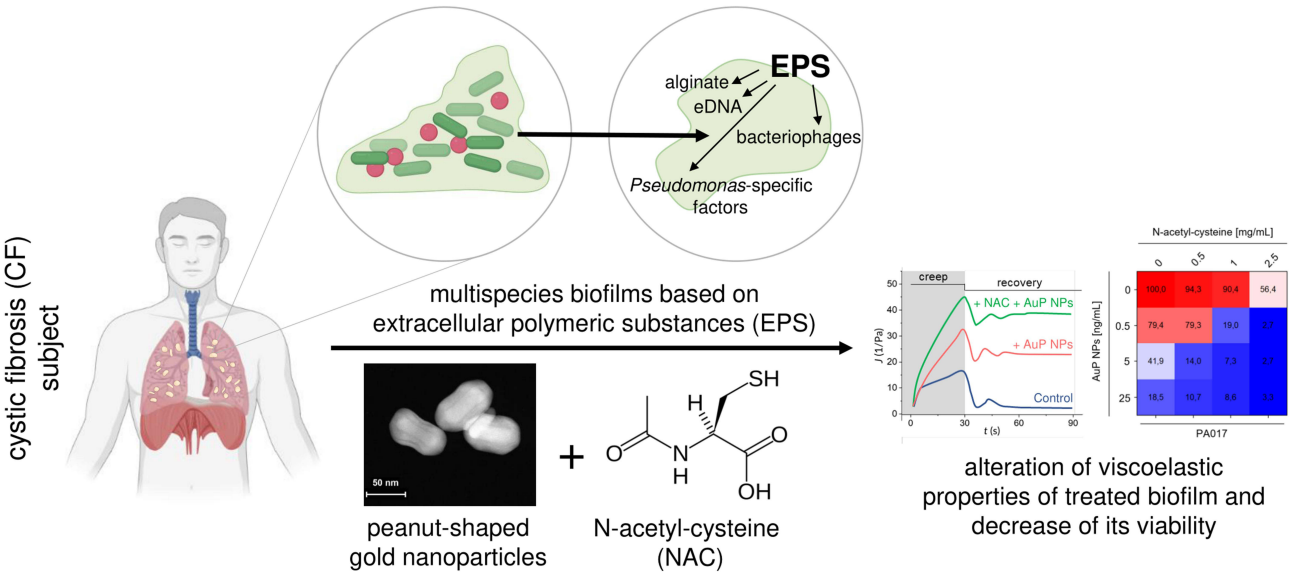

intravenous or inhaled antibiotic therapies, the efficient treatment of pulmonary infections is considerably hampered mostly by the intrinsic or acquired resistance of *P. aeruginosa* to a variety of antibiotics,[3] which is reinforced by its ability to produce drug-resistant biofilms. The latter is defined as three-dimensional communities of bacteria enclosed and protected by a self-produced extracellular polymeric substance (EPS) matrix, composed of polysaccharides (alginate), lysed cell debris proteins, lipids, extracellular DNA (eDNA), and bacteria-specific factors.[4] Importantly, bacteria growth within biofilm in CF lungs is associated with their adaptation to antibiotics used frequently in the therapy of reoccurring pneumonia in CF patients. In this condition, an increased number of mutations associated with antibiotic resistance is generated. Such decreased susceptibility to the applied treatment followed by a lower metabolic rate of biofilm-embedded bacteria and their persistence makes the eradication of biofilms a challenging task.[4] An approach to treat lung infections in patients with CF has evolved beyond antibiotic therapy, with the implementation of various airway clearance techniques (ACTs), in particular mucus thinners, to eliminate excess sputum. This is important not only for improving the patient's condition and final clinical outcomes but also crucial for reducing the microbial burden, as CF sputum components have been proven to promote the development of biofilms.[5] Mucoactive drugs are successfully employed to improve airways clearance and to reduce infection and inflammation.[6,7] Among several mechanisms utilized by mucus thinners,[6] targeting of the biofilm EPS is one the most clinically relevant. Since the EPS matrix not only contributes to maintaining biofilm stability and its viscoelastic parameters,[8] but also is responsible for inactivating exogenous antibiotics and endogenous antimicrobial agents produced by the immune system,[9] its dissolution results in improved susceptibility to biofilm-disrupting agents, as well as environmental, mechanical factors.[10] For this reason, targeting EPS became a favorable approach in the treatment of biofilm-associated medical conditions.

N-acetyl-cysteine (NAC) is a clinically-relevant mucolytic used for biofilm eradication and to facilitate sputum clearance from CF lungs.[11] NAC decreases the biofilm mass of bacterial pathogens[11,12] by (i) disrupting disulfide bonds in mucus, (ii) inhibition of cysteine use by bacteria, and (iii) reduction of EPS matrix production.[11,13] NAC acts synergistically with conventional antibiotics in biofilm eradication.[14] Similarly, pre-treatment of biofilms and CF sputum with NAC improves penetration of some antibiotics and nanoparticles, improving their therapeutic effectiveness.[15–17] In line with this observation, we aimed to elucidate how the employment of this EPS-targeting component might modulate the anti-biofilm activity of varied-shaped gold nanoparticles recently developed and described as effective antimicrobial agents with MIC activity in the

nanogram range.[18,19] An ever-growing number of studies demonstrate that gold nanoparticles have many advantages that allow them to be used in biomedical applications, including easy-controlled synthesis allowing to obtain Au NPs with adjusted size and surface chemistry, as well as relatively low toxicity and controllable biodistribution.[20] We recently demonstrated that due to the ability to induce excessive reactive oxygen species (ROS) production, the disruption of microbial membranes, and leakage of intracellular content, non-spherical gold nanomaterials are highly efficient antimicrobial agents with potential to be used as antimicrobial coatings of medical devices,[18] effective antifungals[19] or drug-delivery carriers.[21] These nanoparticles are effective against *E. coli* and *Candida* biofilms,[18,19] both by decreasing biofilm viability and by limiting adhesion of pathogenic cells to the abiotic surfaces, which is crucial for biofilm formation.[19] Considering these data, we investigated whether non-spherical nanoparticles would be an alternative for the eradication of CF-associated *Pseudomonas* biofilms. Although *P. aeruginosa* is a key bacterial pathogen in progressive and severe CF lung infections, airway pathways of CF subjects are also colonized by multiple bacterial and fungal species with biofilm-forming abilities, and therefore mixed, multi-species biofilms are common in CF lungs.[22] This discovery additionally encourages the usefulness of novel, varied-shaped nanoparticles, which are efficient against both bacterial and fungal pathogens.[18,19]

For the purpose of this study, we chose gold nanostructures with the most promising killing parameters and tested them against 10 clinical strains of *P. aeruginosa* isolated from cystic fibrosis patients. For this purpose, nanoparticles in the shape of peanuts (AuP NPs), stars (AuS NPs), and spherical-like porous nanoparticles (AuSph [70C] NPs), which are characterized by crystalline structure, a varied size ranging from ~45 nm for AuSph (70C) NPs to ~240 nm for AuS NPs and a positive surface charge in a broad pH range were selected. We demonstrate that these nanoparticles, particularly those, which are peanut-shaped, are active against mono- and mixed-species biofilms, including those formed by bacterial and fungal pathogens. Simultaneous treatment of biofilms with EPS-targeting NAC improved the nanoparticles' anti-biofilm abilities, possibly due to better access of AuP NPs to the bacteria. Both of these agents decreased the viscosity of bacterial biofilms, which would be favorable not only for mechanical removal of biofilms but also for easier penetration of other molecules (including antibiotics) into the biofilm's matrix. Additionally, synergistic activity of peanut-shaped gold nanoparticles with tobramycin was observed. To the best of our knowledge, this is one of the few studies presenting the possibility of modulating the anti-biofilm activity of non-spherical nanoparticles using EPS targeting molecules, and the first study demonstrating the ability of gold nanoparticles to alter the rheological properties of bacterial biofilms. Our results encourage further research on the employment of non-spherical gold nanoparticles as possible therapeutic interventions for CF lung infections.

Materials and Methods

Bacterial Strains

P. aeruginosa strains (n = 10) were isolated from the sputum of cystic fibrosis patients attending the Adult Cystic Fibrosis Center, University of Pennsylvania Health System, USA. Sputum samples and bacterial isolates were collected under the approval of The University of Pennsylvania's Institutional Review Board (IRB) (no. 803255) in accordance with the Declaration of Helsinki and written informed consent was obtained from each patient (Table 1). Determination of antibiotic susceptibility of *P. aeruginosa* isolates was performed using the VITEK®2 Compact system and Gram-negative Susceptibility Cards (AST-N331, bioMérieux, Marcy-l'Etoile, France) according to the manufacturer's guidelines, and the results were interpreted using EUCAST ver. 11 clinical breakpoints (Table 2). Clinical strains of *Staphylococcus aureus* (n = 5) and *C. albicans* (n = 5) were obtained from the collection of Department of Medical Microbiology and Nanobiomedical Engineering (Medical University of Bialystok, Poland).

Synthesis and Physicochemical Characterization of AuP NPs, AuS NPs, and AuSph (70C) NPs

Gold nanoparticles in the shape of peanuts (AuP NPs) and stars (AuS NPs), as well as spherical, porous nanoparticles, were synthesized using the CTAB-assisted seed-mediated method as previously described.[18,19] In this synthesis method, CTAB and $AgNO_3$ solutions, which can give antibacterial and antifungal properties, were used for the purpose of AgBr complex formation, which is deposited on one of the crystallographic planes, and therefore nanoparticles grow only in

Table 1 Clinical Characteristic of Cystic Fibrosis Patients from Which *Pseudomonas aeruginosa* Strains Used for Anti-Biofilm Studies Were Isolated

	Sex	Age	Mutation	Antibiotic Treatment	Pulmozyme	Microbes In Sputum*
PA004	F	24	ΔF508*2	–	Yes	–
PA011	F	31	ΔF508*2	Azithromycin, tobramycin	Yes	*Aspergillus*
PA017	F	22	ΔF508*2	Colistin, tobramycin, meropenem, ceftazidime, azithromycin, ciprofloxacin, sulfamethoxazole/trimethoprim	Yes	–
PA024	F	22	ΔF508*2	Tobramycin, meropenem, ceftazidime, sulfamethoxazole/trimethoprim, azithromycin	Yes	–
PA027	M	28	DF508/ W1282X	Tigecycline, cefoxitin, amikacin, azithromycin	Yes	–
PA029	M	27	DF508 N1303K	Tobramycin	–	*S. aureus*
PA030	M	32	W1282X2	Ciprofloxacin	Yes	*S. aureus* (MRSA)
PA038	M	30	TBD	Tobramycin, doxycyclinum	Yes	–
PA039	F	22	ΔF508*2	Azithromycin, sulfamethoxazole/trimethoprim, aztreonam, ceftazidime, meropenem, tobramycin	Yes	*Aspergillus fumigatus*
PA060	F	27	ΔF508*2	–	–	–

Note: *Other than *Pseudomonas aeruginosa.*

Table 2 Antibiotic Sensitivity of *Pseudomonas aeruginosa* Strains Isolated from Cystic Fibrosis Patients. Antimicrobial Susceptibility of *Pseudomonas* Strains Used in This Study Was Estimated Using VITEK® 2 AST-N331 Cards Designated for VITEK®2 Compact System

	TIC/ CLA	PIP	PIP/ TAZ	CFZ	CFP	AZT	IMP	MRP	AMC	GNM	TBR	CPF	LVF	COL	MDR/ XDR
PA004	S	I	S	S	S	S	S	S	I	R	S	R	S	S	Not MDR
PA011	S	I	S	S	S	S	S	S	I	S	S	S	S	S	Not MDR
PA017	R	R	R	R	R	R	R	R	R	R	R	R	R	S	XDR
PA024	R	R	R	R	R	R	R	R	R	R	R	R	R	S	XDR
PA027	S	I	N/A	S	S	S	S	S	S	S	S	S	S	S	Not MDR
PA029	R	R	R	R	S	R	R	R	R	R	R	R	R	S	XDR
PA030	S	I	S	S	S	S	S	S	S	S	S	R	R	S	Not MDR
PA038	S	I	S	S	S	S	S	S	S	S	S	S	S	S	Not MDR
PA039	R	I	S	S	S	S	S	S	S	S	S	S	S	S	Not MDR
PA060	R	R	R	S	S	S	S	S	S	S	S	S	S	S	Not MDR

Notes: Antibiotics against which the tested bacterial strains showed resistance, as well as strains with the XDR phenotype were marked in red.
Abbreviations: TIC/CLA, Ticarcillin/Clavulanic acid; PIP, Piperacillin; PIP/TAZ, Piperacillin/Tazobactam; CFZ, Ceftazidime; CFP, Cefepime; AZT, Aztreonam; IMP, Imipenem; MRP, Meropenem; AMC, Amikacin; GNM, Gentamicin; TBR, Tobramycin; CPF, Ciprofloxacin; LVF, Levofloxacin; COL, Colistin; S, Sensitive; R, Resistant; I, Intermediate.

a specific direction (Supplementary Figure 1).[23–27] To eliminate the impact of those agents, gold nanoparticles were rinsed three times in water followed by centrifugation at 15,000 rpm for 15 minutes and the final product was suspended in water until microbiological tests. As we evidenced by energy-dispersive X-ray spectroscopy (EDS) and presented accordingly in Supplementary Figure 1, silver nanoparticles or silver ions were not present in obtained gold nanoparticles solutions. Furthermore, enhanced FT-Raman spectra of CTAB and Au NPs which were recorded after the rising of synthesized product in water showed a very weak signal from CTAB, which confirms that only a residual amount of CTAB stabilizing the nanoparticles was in the solution.[18] The morphology of synthesized nanoparticles was confirmed using high-angle annular dark-field scanning transmission electron microscopy (HAADF-STEM) and size distribution was recorded based on 100 nanoparticles from each sample tested. Furthermore, to obtain information about the volume of nanoparticles in the *P. aeruginosa* single cell, Nanolive 3D microscope CX-A holotomographic microscope with gridscan 3×3 was used. For this purpose, after imaging of nanoparticles-treated bacteria, a reconstruction of the image was made, marking the areas of nanoparticles in *P. aeruginosa* and the *P. aeruginosa* themselves (Supplementary Figure 2). Then, the volume of *P. aeruginosa* and nanoparticles in the image after 30 minutes of incubation was calculated. Consequently, the volume of all analyzed *P. aeruginosa* cells was 9809.05 μm^3, while nanoparticles occupied the volume of 2667.07 μm^3 (only 3.7 times less than *P. aeruginosa*), which means that there were 0.23 μm^3 nanoparticles in one *P. aeruginosa* (0.86 μm^3).

Antimicrobial Activity of Varied Shaped Gold Nanoparticles Against Planktonic *P. aeruginosa*

To estimate the antipseudomonal potential of AuNPs with various shapes, *P. aeruginosa* isolates were screened using a colony counting assay using a previously published protocol.[28,29] The results were verified by MIC determination using broth microdilution in LB medium (BioMaxima; Lublin, Poland) with AuNPs concentrations ranging from 0.078 to 40 ng/mL. MIC values were recorded visually as the lowest concentration of nanoparticles showing no bacterial growth after 18 h of incubation at 37°C.

Determination of Anti-Biofilm Activities of Nanoparticles

A modified resazurin-based viability assay was used to estimate the capability of AuNPs to prevent biofilm formation by *P. aeruginosa* strains. Accordingly, bacterial isolates at the logarithmic phase of growth were suspended in LB broth at an optical density (OD) of ~ 0.1, distributed into black 96-well flat-bottom plates, and mixed with AuP NPs, AuS NPs, and AuSph (70C) NPs at doses of 0.5, 5 and 25 ng/mL to a final volume of 200 µL and incubated for 72 hours at 37°C. Next, planktonic bacteria were removed by gentle double washing with PBS followed by the addition of resazurin (Sigma-Aldrich, Saint Louis, USA) at a final concentration of 200 µg/mL. After 1 hour of incubation, the viability of biofilms was estimated by recording fluorescence intensity at 520/590 nm excitation/emission wavelengths using a Varioskan Lux microplate reader (Thermo Fisher Scientific, Waltham, USA). EC50% preventive values (effective concentrations resulting in an inhibitory effect in 50% of the bacterial population) were estimated from interpolation of dose-response curves for the various AuNPs. Finally, the anti-biofilm effects were confirmed by fluorescence microscopy using SYTO9/PI double staining of 72 hours biofilms as guided by the manufacturer of the LIVE/DEAD BacLight Bacterial Viability Kit (Invitrogen, Carlsbad, USA).

The Activity of Nanoparticles Against Multi-Species Biofilms

To measure the anti-biofilm activity of AuNPs against dual-species biofilms, ie *P. aeruginosa* – *S. aureus* and *P. aeruginosa* – *C. albicans*, microbes at the logarithmic phase of growth were suspended in LB broth at OD ~ 0.1 and mixed 1:1, then distributed into black 96-well flat-bottom plates supplemented with AuP NPs, AuS NPs and AuSph (70C) NPs at doses of 0.5, 5 and 25 ng/mL to a final volume of 200 µL, and incubated for 72 hours at 37°C prior to resazurin-based staining and fluorescence analysis as described above.

Investigation of Anti-Biofilm Effects of Varied Shaped AuNPs in the Presence of Biofilm-Promoting Factors

The impact of DNA, sodium chloride and magnesium ions on the anti-biofilm activity of AuNPs was quantitatively investigated by the estimation of ED50% preventive values. Briefly, LB broth medium was supplemented with deoxyribonucleic acid from salmon sperm, sodium chloride, or magnesium chloride (Sigma-Aldrich, Saint Louis, USA) to final concentrations of 1 mg/mL, 180 mM, and 1 mM, respectively, and biofilm viability assessment was performed as described.

Evaluation of the Combined Effect of AuP NPs with NAC and Tobramycin

A checkerboard technique was used to explore the combinatory effect of peanut-shaped AuNPs with NAC and tobramycin (Sigma-Aldrich, Saint Louis, USA). For this purpose, *P. aeruginosa* biofilms were formed in the presence of AuP NPs at concentrations of 0.5, 5 and 25 ng/mL and NAC (0.5, 1 and 2.5 mg/mL) or tobramycin (0.125, 0.5 and 1 μg/mL). Relative inhibitory effects of tobramycin or AuP NPs were calculated as the difference between single and combined treatments.

Assessment of Biofilm Viscoelastic Properties

Rheological properties of the *P. aeruginosa* biofilm exposed to NAC and AuP NPs were investigated using a Haake Rheostress 6000 rheometer (Thermo Scientific, USA) in a plate-plate arrangement, wherein the diameter of the upper plate was 20 mm. All tests were performed at 21°C. To perform the measurements, *P. aeruginosa* PA024 biofilm samples (prepared by inoculation of 10 mL LB broth medium with an overnight culture of PA024 and further incubation in 90-mm Petri dishes for 10 days at 37°C) were treated with NAC (2.5 mg/mL), AuP NPs (25 ng/mL) or NAC/AuP NPs mixture, gently pipetted and spread on the lower plate of the rheometer. To the control samples, an equal volume of PBS was added in the place of NAC/AuP NPs. The bottom plate was then raised into the 1 mm gap between the plates, which corresponds to a volume of 400 μL. To determine the viscous properties of the biofilm, rotational tests were carried out, by continuous rotation of the upper plate at a shear rate γ in the range 0.1–100 1/s (increasing logarithmically). Based on the recorded shear stress τ in the sample, the dynamic viscosity η (1) was determined as a function of the shear rate:

$$\eta = \frac{\tau}{\dot{\gamma}}$$

The creep-recovery test was used to determine viscoelastic properties. In the test, the biofilm sample was subjected to continuous shear stress of 0.1 Pa for 30s, followed by stress removal for another 60s, during which the shear strain was measured. Based on the shear stress and the shear strain in the sample, the compliance (2) was calculated as a function of time:

$$J(t) = \frac{\gamma(t)}{\tau}$$

Statistical Analysis

Data are presented and mean ± SE. The significance of differences was determined using the two-tailed Student's *t*-test. Statistical analyses were performed using OriginPro 2021 (OriginLab Corporation, Northampton, USA). $p<0.05$ was considered to be statistically significant.

Results

Morphology and Size Distribution of Synthetized Nanoparticles

For the purpose of this study, gold nanoparticles were prepared using CTAB-assisted seed-mediated method according to the protocols presented in our previous papers.[18,19] To confirm the morphology of developed nanomaterials, HAADF-STEM analysis was performed. As demonstrated in Figure 1, a set of nanoparticles with different morphology (peanut-shaped, star-shaped and spherical-like porous nanoparticles; Figure 1A) and size distribution (Figure 1B) was obtained. Accordingly, non-aggregated peanut-like gold nanoparticles, which have rod-like shape core had size ~60 nm. Star gold

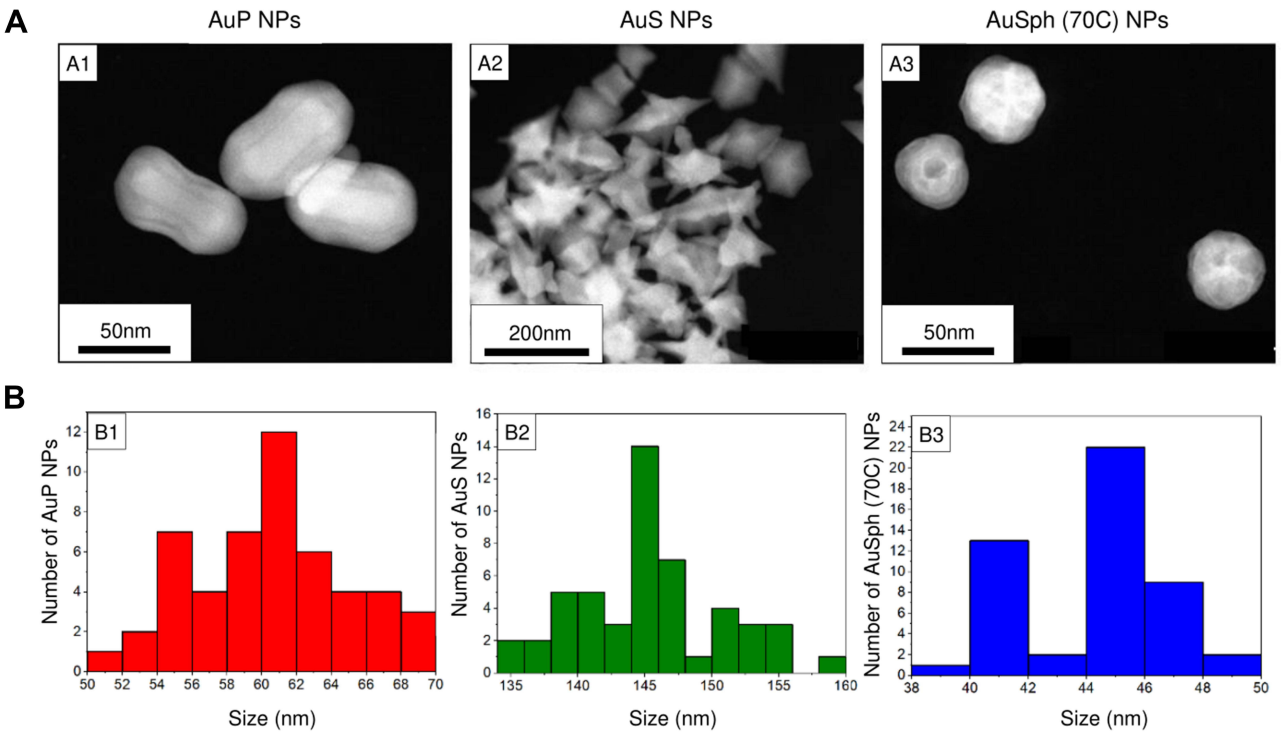

Figure 1 Physicochemical properties of the developed gold nanopaenuts (AuP NPs; panels A1 and B1), gold nanostars (AuS NPs; panels A2 and B2) and spherical, porous nanoparticles (AuSph (70C) NPs; panels A3 and B3). High-angle annular dark-field scanning transmission electron microscopy (HAADF-STEM) overview (**A**). Size distribution of obtained Au NPs is presented in (**B**).

nanoparticles were characterized by a different size of arms – average size was calculated as ~144 nm, although at the farthest ends of the stars' arms their size varied. Size of spherical gold nanoparticles with porosity structure also was recorded as ~44 nm on average. All nanoparticles did not form aggregates and created monolayer. At the same time, comparison of these three kind of Au NPs revealed that the AuS NPs were the least dispersed.

Nanoparticles Exert Antimicrobial Activity Against Clinical Multidrug-Resistant Isolates of *P. aeruginosa*

All *P. aeruginosa* strains under study were isolated from the sputum of cystic fibrosis subjects. Clinical characteristics of patients are shown in Table 1. All isolates were non-susceptible to antipseudomonal ureidopenicillin – piperacillin, and according to the classification of antimicrobial resistance,[30] three of them (30%) (ie PA017, PA024, and PA029) were recognized as extensively-resistant (XDR) and colistin-only-sensitive (COS), ie, resistant to all antipseudomonal agents, namely, penicillins, cephalosporins, carbapenems, monobactams, fluoroquinolones, and aminoglycosides, except colistin (Table 2). Furthermore, three strains showed resistance/non-susceptibility to at least one member of the fluoroquinolone (PA030) and aminoglycoside class (PA011) or both (PA004), and additional two strains (PA039 and PA060) were resistant to ≥ 1 antipseudomonal penicillin, including combinations with β-lactamases inhibitors (Table 2). As presented in Figure 2, all tested nanoparticles exert potent bactericidal activity against these *P. aeruginosa* strains even at a dose of 1 ng/mL, as estimated using the colony counting assay. All tested isolates exert similar susceptibility to AuNPs, despite a variety of drug resistance profiles and different phenotypes. This uniform antipseudomonal activity was preserved in a highly nutritious Luria-Bertani (LB) medium since the minimal inhibitory concentration (MIC) for AuP NPs and AuS NPs varied by just one dilution between all *P. aeruginosa* strains and for all but two isolates for AuSph (70C) NPs (Table 3). However, in this case, the concentration of AuNPs must be elevated to at least 20 ng/mL.

Such potent activity of the nanoparticles synthesized for the purpose of this study might be associated with the presence of residual CTAB on their surface, nevertheless, we excluded such possibility with experimental tests. Firstly, a lack of significant antipseudomonal activity of CTAB alone (MICs >32 μg/mL for all tested isolates; Supplementary Table 1) was observed. Since the efficiency of drugs might be drastically increased upon their attachment to the surface

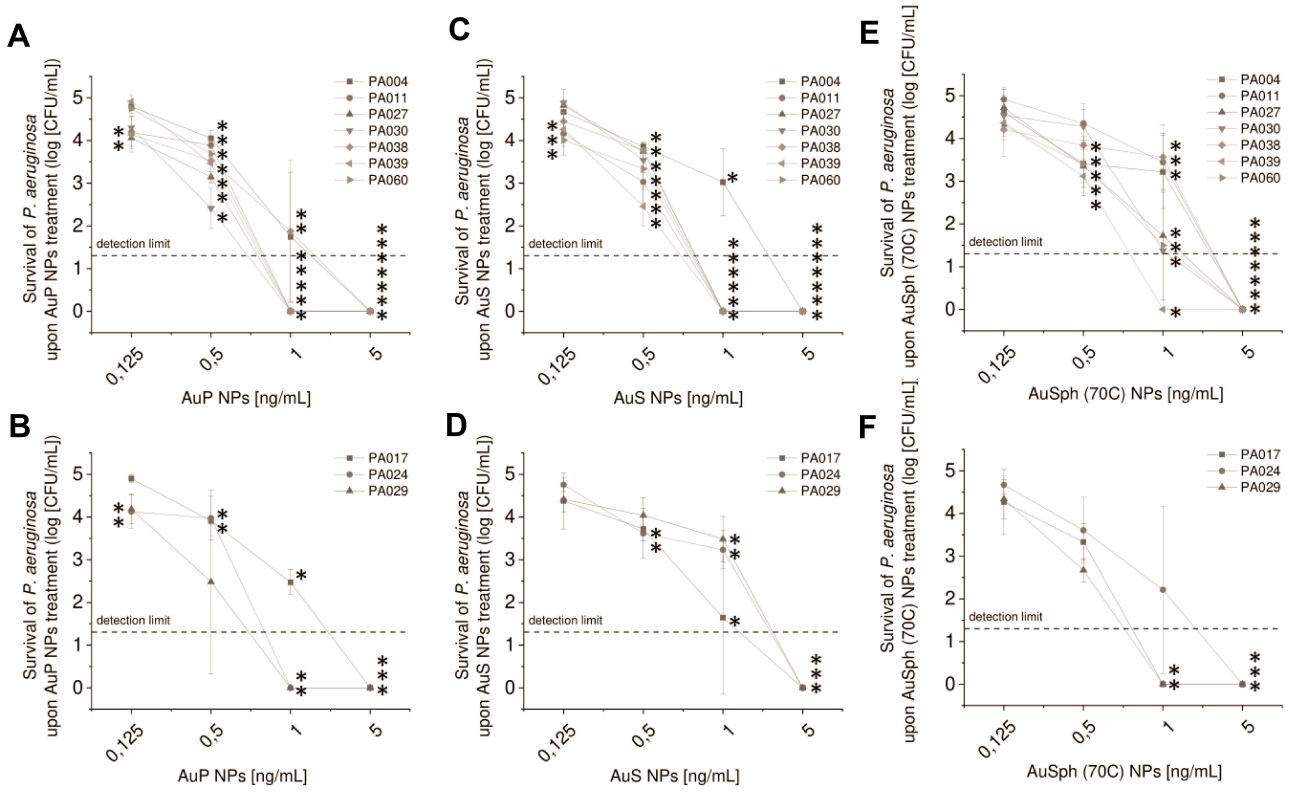

Figure 2 Bactericidal activity of gold nanoparticles having the shape of peanuts (AuP NPs; (**A** and **B**)), stars (AuS NPs; (**C** and **D**)) and spherical, porous nanoparticles (AuSph (70C) NPs; panels E-F) against 10 clinical strains of *P. aeruginosa* isolated from the sputum collected from the lung of cystic fibrosis patients. Strains were divided into non-MDR (**A, C** and **E**) and MDR-strains (**B, D** and **F**). Results are presented as mean ± SD. *Indicates statistical significance ($p<0.05$) when compared to untreated control.

of nanomaterials when compared to the free form, additional control consisting of spherical nanoparticles coated CTAB was provided. Accordingly, AuNPs appear to be superior to spherical AuNPs, since control gold nanospheres, which were both unfunctionalized or cetrimonium bromide (CTAB)-modified were inactive up to a dose of 2 μg/mL, ie, the

Table 3 Minimal Inhibitory Concentrations (MIC; Ng/mL) of Peanut-Shaped (AuP NPs), Star-Shaped (AuS NPs) and Porous Spherical-Like Gold Nanoparticles [AuSph (70C) NPs] Against Clinical Strains of *Pseudomonas aeruginosa* Isolated from Patients with Cystic Fibrosis

	AUP NPS [NG/ML]	AUS NPS [NG/ML]	AUSPH (70C) NPS [NG/ML]
PA004	40	40	>40
PA011	20	20	20
PA017	20	20	40
PA024	40	40	20
PA027	40	40	40
PA029	20	40	40
PA030	20	20	40
PA038	40	40	>40
PA039	40	40	40
PA060	40	40	40

highest concentration tested (Supplementary Table 1). This is in agreement with our previous report, demonstrating the lack of antipseudomonal activity of spherical nanomaterials.[18] Collectively, those data suggest that virtually all observed antibacterial effects can be ascribed to the morphology of AuNPs.

Nanoparticles Inhibit the Formation of *P. aeruginosa* Biofilms

As demonstrated in Figure 3, 50% inhibition of biofilm formation in all tested isolates by the AuNPs was observed in a concentration range from 3.9 ± 0.6 to 34 ± 10 ng/mL, with an average effective, 50%-level concentration (EC50%) for AuP NPs, AuS NPs and AuSph (70C) NPs of 8.7 ± 1.1, 12.4 ± 2.3 and 12 ± 2.7 ng/mL, respectively. Although differences among different nanoparticles did not reach statistical significance (p = 0.1697 when comparing peanut- and star-shaped gold nanoparticles), AuP NPs seemed to be the most active against drug-resistant strains. For PA017, PA024 and PA029 strains the lowest EC50% concentrations (8.75 ± 2.50, 10.08 ± 2.14 and 15.98 ± 3.20, respectively) were recorded for AuP NPs-treated samples, while the highest ones (9.49 ± 1.24, 15.72 ± 5.09 and 33.53 ± 10.23 ng/mL) were detected when biofilms were formed in the presence of porous, spherical-like nanoparticles (Figure 3A). To visualize the structure and viability of AuP NP-treated biofilms, we performed fluorescence microscopy using SYTO9 and propidium iodide (PI) dual staining. As demonstrated in Figure 3B, when AuP NPs are applied prior to initiation of biofilm, the signal from both viable and dead bacterial cells is significantly lower, which indicates that the formation of biofilm, and thus its mass, is considerably inhibited.

Nanoparticles Strongly Inhibit the Formation of Multi-Species Biofilms

Since in the lungs of CF patients *P. aeruginosa* often coexist and interacts with other microbes, including bacteria (*S. aureus)* and fungi (*C. albicans)*,[22] we decided to assess whether our nanoparticles are able to inhibit the formation of dual-species biofilms composed of *P. aeruginosa* mixed with *S. aureus* or *C. albicans* cells. As presented in Figures 4A-F, nanoparticles inhibit mixed biofilms formation. This effect seems to be more prominent for *S. aureus/P. aeruginosa* combinations than for

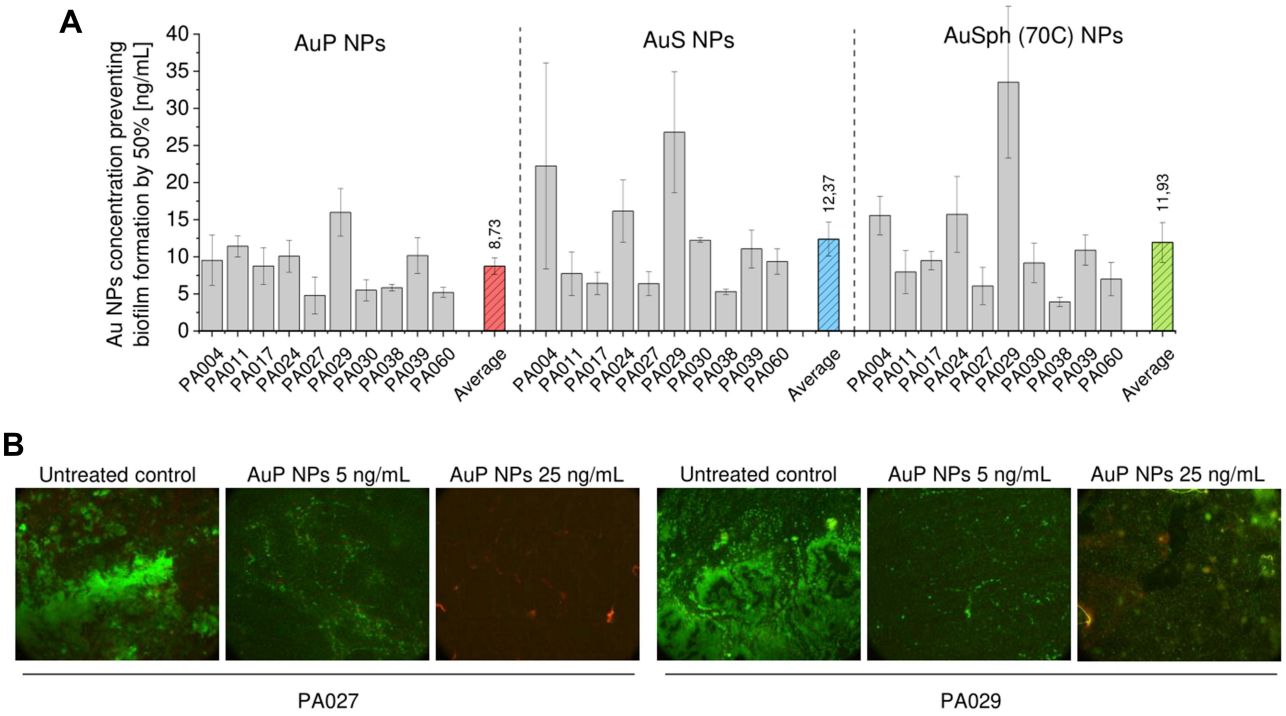

Figure 3 Anti-biofilm activity of gold nanoparticles having the shape of peanuts (AuP NPs), stars (AuS NPs) and spherical, porous nanoparticles (AuSph (70C) NPs) against 10 clinical strains of *P. aeruginosa* isolated from sputum collected from the lung of cystic fibrosis patients. The ability of the tested nanoparticles to prevent biofilm formation (**A**) was investigated using resazurin staining. Au NPs concentration required to prevent biofilm formation by 50% was calculated from interpolation of dose-response curves recorded for each nanoparticles tested. Live/dead staining of biofilms formed and disrupted upon incubation with AuP NPs at doses of 5 and 25 ng/mL is presented in (**B**). Green color indicates SYTO9-positive viable cells, red color – PI-positive dead cells. For (**A**), the results are shown as mean ± SE. For (**B**), the results from one representative experiment are shown.

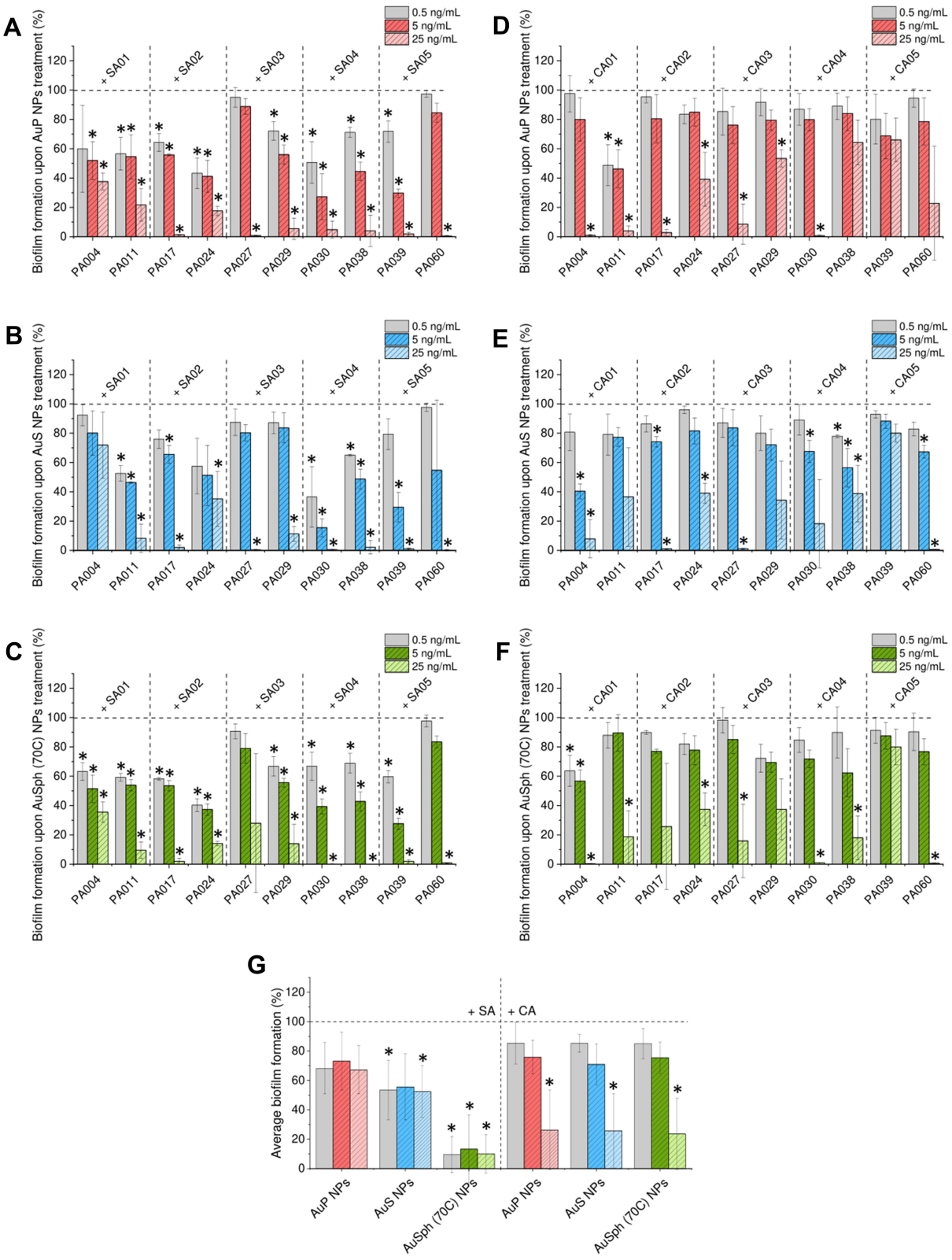

Figure 4 Anti-biofilm activities of gold nanoparticles having the shape of peanuts (AuP NPs), stars (AuS NPs) and spherical, porous nanoparticles (AuSph (70C) NPs) against multispecies biofilms. Decreased formation of biofilms by *P. aeruginosa* mixed with *S. aureus* (SA) isolates or *P. aeruginosa* mixed with *C. albicans* (SA) isolates upon treatment with tested nanoparticles at doses of 0.5, 5 and 25 ng/mL is presented in (**A**–**C**) and (**D**–**F**), respectively. (**G**) demonstrates the formation of mixed biofilms calculated as average from 10 tested *P. aeruginosa* strains. The results are presented as mean ± SE. *Indicates statistical significance ($p<0.05$) when compared to untreated control.

those containing fungi. As shown in Figure 4G, the average viability of dual-species biofilms formed in the presence of 25 ng/mL AuNPs is 10.97% (when the second microbe is *S. aureus*) and 25.49% (when the second microbe is *C. albicans*).

DNA and High Salt Concentration, but Not Magnesium Ions Affect the Anti-Biofilm Abilities of Gold Nanoparticles

In order to achieve satisfactory therapeutic efficiency in cystic fibrosis lung, it is crucial to maintain the antimicrobial effect, in the presence of factors occurring in excessive amounts in this medical condition. Among a variety of factors decreasing the killing efficiency of conventional antibiotics,[31] DNA, sodium chloride (NaCl), and magnesium ions (Mg^{2+}) are among the most clinically relevant. As demonstrated in Figure 5A, a considerable variation in anti-biofilm activity among AuP NPs, AuS NPs, and AuSph

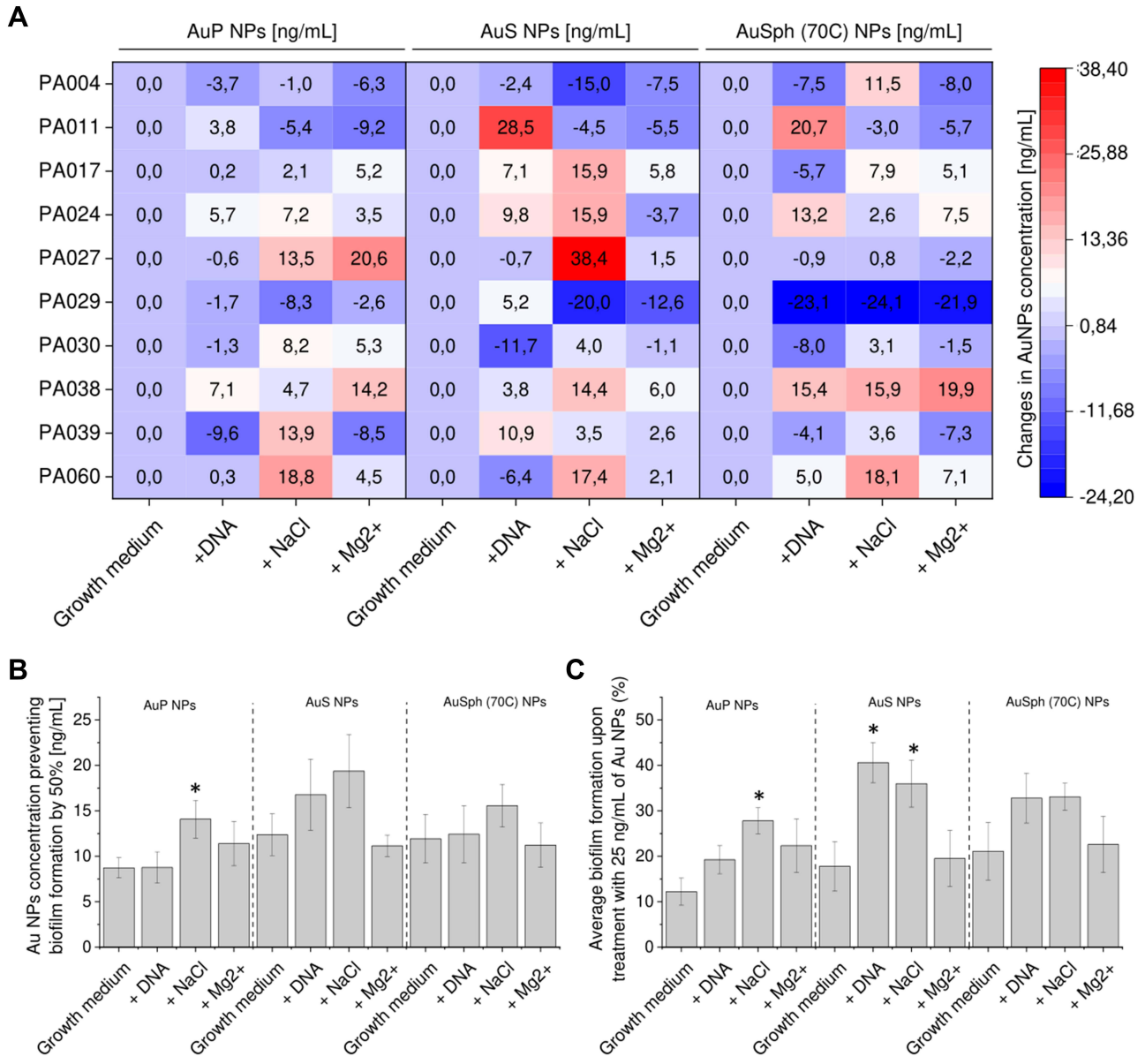

Figure 5 Ability of gold nanoparticles having the shape of peanuts (AuP NPs), stars (AuS NPs) and spherical, porous nanoparticles (AuSph (70C) NPs) to prevent formation of biofilms by *P. aeruginosa* in the presence of biofilm-promoting factors: 1 mg/mL DNA, 180 mM sodium chloride (NaCl, ionic strength $I = 0.18$) or 1 mM magnesium divalent ions (Mg^{2+}, $I = 0.002$). Au NPs concentration required to prevent biofilm formation by 50% (EC50%) was calculated from interpolation of dose-response curves recorded for each nanoparticles tested. Alterations in EC50% for each tested strain are presented in (**A**) using heatmap plot with red and blue colors indicating the increase and decrease of EC50%, respectively, when compared to biofilms formed in LB medium without supplements. The average EC50% for all tested *P. aeruginosa* strains and average biofilm formation upon treatment with 25 ng/mL of Au NPs are presented in (**B** and **C**). The results are presented as mean ± SE. * indicates statistical significance ($p<0.05$) when compared to untreated control.

(70C) NPs was observed in the presence of NaCl followed by DNA, but not in the tested range of Mg^{2+} concentration. In detail, the higher salt content resulted in a considerable increase of EC50% and biofilm formation for all tested nanoparticles, however, this effect was most visible for AuS NPs at 25 ng/mL (36 ± 5%) (Figure 5C). Interestingly, magnesium ions did not considerably interfere with the anti-biofilm activities of any tested nanoparticles. Since we hypothesized that this salt-dependent phenomenon may result from alterations in NPs affinity to the negatively-charged bacterial membranes, additional analyses focused on the AuNPs' zeta potential (ZP). Accordingly, we noted that for all tested nanoparticles a significant decrease of the ZP value was recorded, while this effect was far stronger when NaCl ($I = 0.18$) was added than magnesium chloride ($I = 0.003$). More precisely, the ZP value of AuP NPs, AuS NPs and AuSph (70C) NPs dropped from +34.25, +42.63 and +36.59 mV to +14.94, +13.38 and +0.52 mV, respectively when NaCl ($I = 0.18$) was added. At the same time, supplementation with Mg^{2+} ($I = 0.002$) changed the surface charge of nanoparticles to +29.12, +14.62 and +18.15 mV. These results suggest that alterations in the surface chemistry of nanoparticles might indeed determine the decreased ability to eradicate bacterial biofilms. On the other hand, the presence of DNA did not significantly affect the activity of AuP NPs and AuSph (70C) NPs – their average effective 50%-level concentrations increased from 8.73 ± 1.11 to 8.76 ± 1.72 ng/mL (p=0.9875) and from 11.93 ± 2.68 to 12.43 ± 3.15 ng/mL (p=0.9064), respectively (Figures 5B and C). In contrast, the impact of DNA on both anti-biofilm parameters of AuS NPs was more pronounced (Figure 5B and C). ED50% increased by 36%, ie, from 12.37 ± 2.29 to 16.77 ± 3.91 ng/mL (p = 0.3449), while the biofilm viability increased by 2.3-fold, ie, from 17.77 ± 5.45 to 40.62 ± 4.43% (p = 0.0044). Based on these results, peanut-shaped nanoparticles appear to be most active against *P. aeruginosa* biofilms and most resistant to inhibitory effects related to CF sputum compounds. They were used for further experiments focused on synergistic interactions of gold nanoparticles with NAC and tobramycin, as well as their influence on viscoelastic parameters of *P. aeruginosa* biofilms (see below).

The Anti-Biofilm Effect of Gold Nanopeanuts is Potentiated by NAC

One of the reasons for the resistance of biofilm-embedded bacteria to the applied treatment is the failure of some antibiotics (including aminoglycosides and fluoroquinolones)[32] to penetrate through the biofilm matrix, which makes it impossible to achieve an appropriate therapeutic effect.[33] Based on this, we hypothesize that nanoparticles would be more effective if suitable access to bacteria would be ensured. As presented in Figure 6, NAC substantially enhanced, even by 91% (Figure 6A), the AuP NP-mediated anti-biofilm effect (Figure 6A). A combinatory treatment by peanut-shaped gold nanoparticles and NAC, decreases the effective doses of nanoparticles. For drug-resistant *P. aeruginosa* isolates (Figure 6B), a decrease of PA017 biofilm viability to 19% was observed when 0.5 ng/mL AuP NPs were combined with 1 mg/mL of NAC. In contrast to that, when AuP NPs and NAC were used alone, 79.7% and 90.4% of the biofilm mass was viable. A comparative effect was achieved only when 25 ng/mL gold nanoparticles were used, which is a 50-fold higher dose. Similarly, nearly complete eradication of the biofilm was recorded when this dual treatment was applied against another XDR isolate - PA024 (Figure 6B). These data suggest that combining gold nanoparticles with mucolytics can achieve satisfactory therapeutic effects against biofilms in CF lungs.

Gold Nanopeanuts Decrease the Viscosity of *P. aeruginosa* Biofilms and Act Synergistically with NAC

Having in mind reports indicating the improvement of CF sputum viscosity parameters upon treatment with NAC,[15] and considering the evidence presenting interaction of gold nanoparticles with disulfide bonds, we aimed to explore whether rheological parameters of *P. aeruginosa* biofilms might be altered upon treatment with those compounds. To determine the effects on both elasticity and viscosity, rotational and creep-recovery tests were performed. The addition of both NAC and AuP NPs influenced the rheological properties of the biofilm, which presumably corresponds to structural changes in these matrices. Viscosity curves (Figure 7A) showed that both untreated and treated biofilm samples exhibited non-Newtonian properties. The addition of NAC and AuP causes a significant decrease in viscosity in the range of low shear rates (<1), and no such effect at high shear rates. In order to separate these two shear rate ranges, the values of the zero-shear rate and the infinite-shear rate viscosities (η_0 and η_∞, respectively) were distinguished. As demonstrated in Figure 7B, NAC and AuP NPs, individually and in combination, significantly reduce the biofilm zero-shear rate viscosity (by 26–31%), hence AuP NPs are as effective as NAC in

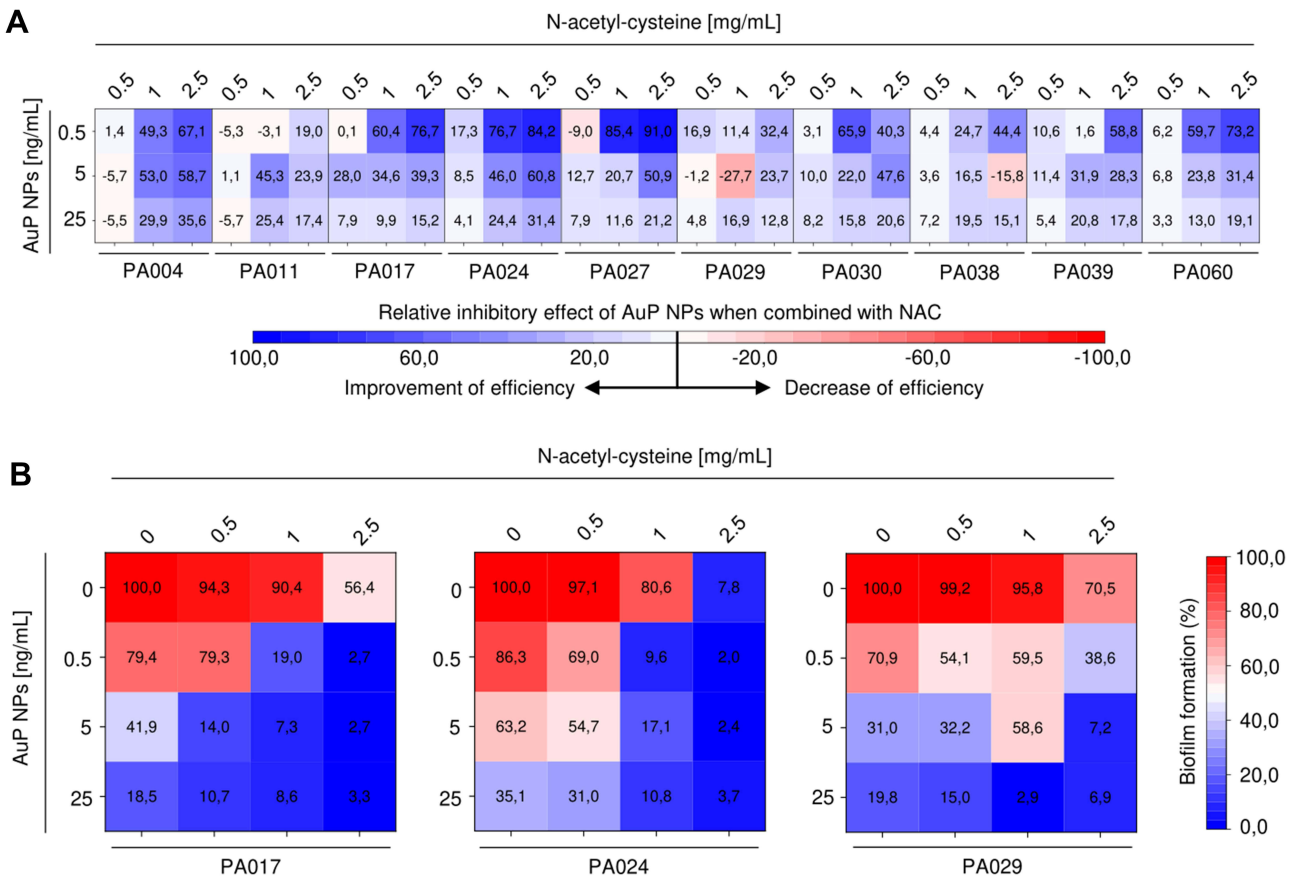

Figure 6 Improvement of therapeutic efficiency of gold nanopeanuts (AuP NPs) in the presence of N-acetyl-cysteine (NAC). Relative inhibitory effect of AuP NPs (at concentrations of 0.5, 5 and 25 ng/mL) when combined with NAC (at doses of 0.5, 1 and 2.5 μg/mL) compared to treatment with AuP NPs alone is presented in (**A**) using heatmap plot type with blue and red colors indicating improvement and decrease of therapeutic efficiency, respectively. (**B**) demonstrates formation of biofilms by three drug-resistant *P. aeruginosa* strains (PA017, PA024, PA029) upon treatment with NAC and AuP NPs alone or when combined. Results are presented as mean from 3 independent replicates.

"thinning" the biofilm. However, we did not observe any enhancement of this effect, when we used both substances simultaneously. These data also show that there is no apparent effect of either NAC or NPs on biofilm infinite-shear rate viscosity. Analysis of creep-recovery curves (Figure 7C) showed that biofilm samples exhibit viscoelastic properties. When stress of 0.1 Pa was applied to them, the measured strain in all samples increased non-linearly, and equilibrium was not reached after 30seconds. During this time, an increase in biofilm compliance, which is the ratio of strain and stress in the sample, was observed. When the stress was removed, the strain of the samples was reduced, consistent with partial elastic recovery. After 60s without the applied stress, the samples did not return to their original state; some of the applied strain remained in the samples, so they are in an unrecovered state (characterized by $J_{t=90s}$). We observed that the addition of NAC and AuP NPs significantly increased the creep compliance J, as presented by the maximum values of creep compliance after 30s ($J_{t=30s}$) (Figure 7D). Upon NAC addition $J_{t=30s}$ value increased more than 2.5 times, upon AuP NPs - more than 2 times, while when they are applied simultaneously $J_{t=30s}$ increased nearly 3 times. To show more clearly the unrecovered strain after creep, the difference in compliance values between the state of maximum compliance and the unrecovered state was related to the value of the maximum compliance (Figure 7D). Values closer to 1 indicate a closer return to the original state, as seen in the control sample. We observed that the addition of NAC and AuP NPs significantly reduces these values, which indicate some changes in the structure of the biofilm and its susceptibility to mechanical factors. These results demonstrate that both NAC and gold nanopeanuts decrease the viscosity and alter viscoelastic properties of treated biofilms, while the effect of NAC is more prominent than that observed for AuP NPs. An additive effect of NAC and gold nanoparticles was also observed.

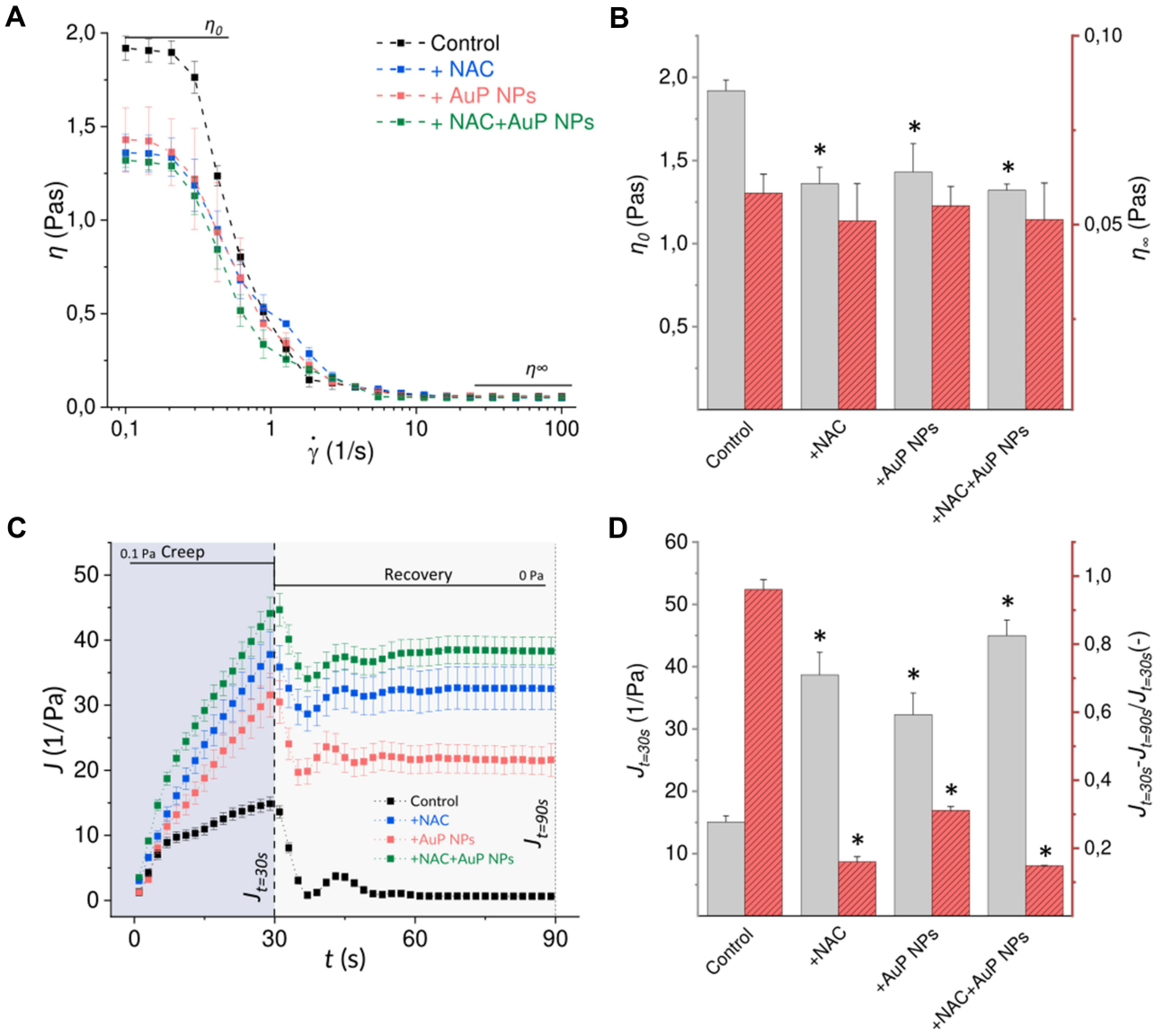

Figure 7 Effects of NAC and AuP NPs on rheological properties of *Pseudomonas aeruginosa* biofilm: (**A**) dynamic viscosity (mean values) as a function of shear rate for control samples, and samples treated with NAC and AuP NPs; (**B**) zero-shear viscosity η_0 and infinity-shear viscosity η_∞ determined from the viscosity curves; (**C**) compliance as a function of time in creep-recovery tests of samples subjected to 0.1 Pa stress; (**D**) mean maximal creep compliance values (at 30s $J_{t=30s}$) and the ratio of difference between $J_{t=30s}$ and unrecovered creep compliance (at 90s $J_{t=90s}$) to maximal creep compliance calculated from creep-recovery curves. * indicates statistical significance ($p<0.05$) when compared to untreated control.

Peanut-Shaped Gold Nanoparticles Improve the Efficiency of Tobramycin Against Tobramycin-Resistant Strains

One of the greatest challenges in the effective treatment of CF lung infections is an ever-growing resistance of pathogenic bacteria, including *P. aeruginosa*, to conventional antibiotics. In our study, three isolates ie PA017, PA024, and PA029 were reported to be insensitive to treatment with all tested antimicrobials, excluding colistin. Given the considerable utility of aerosolized tobramycin in the treatment of CF-associated lung infections,[34] we aimed to investigate whether the presence of gold nanoparticles might improve the efficiency of tobramycin against drug-resistant strains. We hypothesized that the ability of gold nanopeanuts to both display antimicrobial activity and alter the viscoelastic properties of *Pseudomonas* biofilms would be favorable to overcome the insensitivity of CF-derived strains. As demonstrated in Figure 8A, tobramycin efficiency is significantly improved when AuP NPs are present, particularly when low

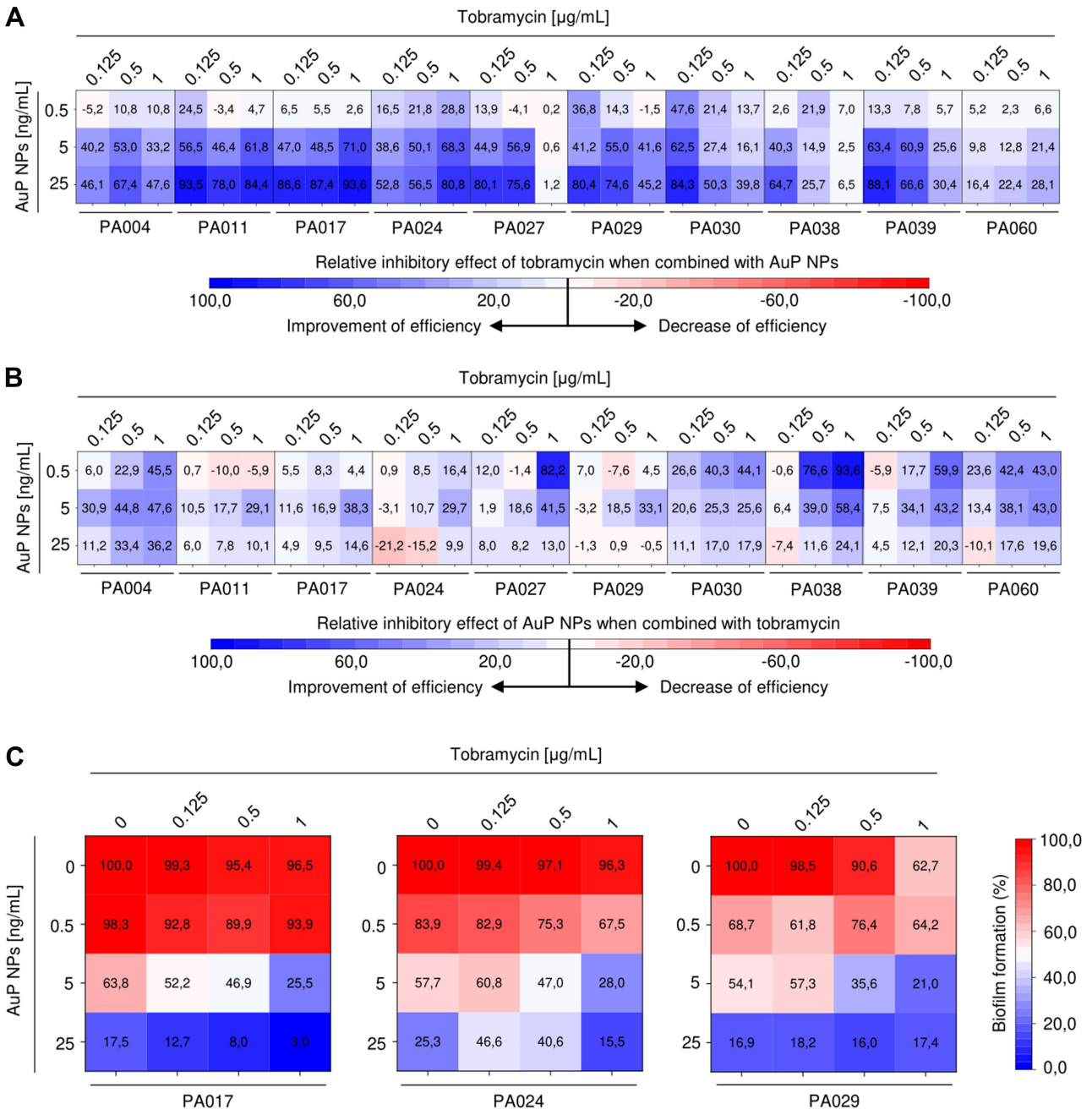

Figure 8 Improvement of therapeutic efficiency of tobramycin and AuP NPs when combined together. Relative inhibitory effect of tobramycin (at concentrations of 0.125, 0.5 and 1 µg/mL) and AuP NPs (at doses of 0.5, 5 and 25 ng/mL) compared to single-agent treatment is presented in (**A** and **B**) using heatmap plot type with blue and red colors indicating the improvement and decrease of therapeutic efficiency, respectively. (**C**) demonstrates the formation of biofilms by three tobramycin-resistant *P. aeruginosa* strains (PA017, PA024, PA029) upon treatment with tobramycin and AuP NPs alone or when combined. The results are presented as mean from 3 independent replicates.

concentrations (0.125–0.5 µg/mL) of tobramycin are employed. Combining tobramycin with AuP NPs limited the formation of *P. aeruginosa* biofilms by an additional 94.2% compared to treatment with tobramycin alone. Combining tobramycin with AuP NPs also decreased the effective concentrations of gold nanopeanuts (Figure 8B). This improvement of anti-biofilm efficiency was particularly pronounced against tobramycin-resistant isolates. As shown in Figure 8C, the decrease of biofilm viability at a higher concentration of AuP NPs (25 ng/mL) resulted mostly from the anti-biofilm activity of gold nanopeanuts themselves. However, at lower doses, a potent combinatorial effect of AuP NPs with tobramycin was observed (Figure 8C). Combining 1 µg/mL of tobramycin with 5 ng/mL of AuP NPs decreased the

formation of PA017 biofilm up to 25.5%, whereas the viability of single-treated biofilms was 96.5% and 63.8% for tobramycin and AuP NPs, respectively. Similarly, combined treatment results in PA029 biofilm formation limitation up to 21%, while for tobramycin and gold nanopeanuts viability was 62.7% and 54.1%. These results indicate that combining tobramycin with gold nanoparticles has the potential to increase the efficiency of antibacterial treatments.

Discussion

Biofilm formation by mucoid (alginate-producing) strains of *P. aeruginosa* is one of the key factors in the development of drug-resistant phenotypes and the persistence of chronic lung infections in cystic fibrosis patients.[35] At the same time, colonization of CF patients by multidrug-resistant strains (MDR) is constantly growing and reaching up to 45% of cases.[36] This motivates seeking novel antimicrobial agents and concurrently targeting bacterial cells and components of their biofilms. In our study, among 10 strains isolated from the sputum of CF patients, 3 (30%) were colistin-only-sensitive (COS), (Table 2). Our initial susceptibility testing performed using a colony counting assay, demonstrated that some classes of gold nanoparticles (Figure 1) are effective against all tested isolates, regardless of their drug sensitivity profile (Figure 2). This strain-independent effect is in agreement with our previous report, where nanogram antimicrobial activity of non-spherical gold nanoparticles was demonstrated as resulting from excessive oxidative stress leading in further steps to permeabilization of the microbe membranes and leakage of intracellular contents.[18,19] Similarly, elongated gold nanoparticles, as well as spherical hybrid silver-gold nanoparticles were reported to induce local stress on the bacterial wall and trigger overproduction of reactive oxygen species (ROS).[37,38] Based on this, we propose that an analogous mechanism is responsible for the non-specific killing efficiency of gold nanoparticles against the clinical strains of *P. aeruginosa* isolated from CF sputum tested here. Importantly, gold nanoparticles were reported to induce resistance to a very limited extent and less than silver nanoparticles.[39,40] A clinically-relevant feature of metallic nanoparticles, particularly gold ones is also their synergistic effects with conventional antibiotics, which improves the antimicrobial efficiency and alleviates drug resistance.[41–43] In this regard, administration of non-spherical gold nanoparticles, particularly peanut shapes, would be favorable because of their powerful killing efficiency itself and potentially, low capability to induce drug resistance. However, the latter should be more thoroughly investigated in the future.

As estimated using microbroth dilution method, AuNPs doses reaching 20–40 ng/mL are required to inhibit the outgrowth of bacteria in LB broth medium (Table 3). Interestingly, although the nanogram antimicrobial efficiency of varied-shaped AuNPs was preserved for *Pseudomonas* isolates, MIC values recorded against other microbes, including *S. aureus, E. coli* or *Candida spp*., were significantly lower (typically not exceeding 1.25 ng/mL).[18,19] We suggest that EPS produced by *Pseudomonas* bacteria are responsible for limiting the killing effectiveness. Considering the differences in the anti-Pseudomonas activity of nanoparticles observed in PBS and LB broth (Figure 2, Table 3), as well as the fact that nanoparticles interact with *Pseudomonas* bacterial membranes similarly to other microorganisms,[18] we believe that the formation of matrix outside the bacteria considerably restrains the successful penetration of nanoparticles and hamper the access of AuNPs to cells' surface. This translates directly into inhibition of anti-biofilm capabilities of tested nanoparticles. Indeed, as we presented, nanomaterials exert activity against biofilms formed by *P. aeruginosa* bacteria (Figure 3), as well as multi-species biofilms co-cultured with *C. albicans* or *S. aureus* (Figure 4), although the satisfactory effect is achievable at relatively higher concentrations of approx. 25 ng/mL. This encourages the optimization of these materials in terms of their interaction with bacteria and the extracellular matrix they produce. This can be achieved both (i) by optimizing the parameters directly related to the biological activity of nanoparticles, and (ii) by combining nanomaterials with other factors modulating the composition and physicochemical properties of the bacteria-derived matrix. Our data support the assumption that modifying nanoparticles in terms of their morphology, particularly size and shape, will affect the effectiveness of NPs in our experimental settings. Notably, when comparing the anti-biofilm activity of synthesized nanomaterials with each other, gold nanopeanuts seemed to be the most active, since effective doses against forming biofilms are in the majority of samples in the concentration range of 5–10 ng/mL (Figure 3). Moreover, AuP NPs-mediated effects are only minimally reduced by the addition of DNA, high salt concentration, or magnesium divalent ions (Figure 5B and C), suggesting a satisfactory anti-biofilm activity in the CF lung environment. We hypothesize that this effect results from the most optimal morphological characteristics of gold nanopeanuts, primary their shape, size, and positively-charged surface,[18] since previous reports already established that those features considerably affect the biofilm penetration and eradication abilities of nanoparticles.[44,45] Using nitric oxide-releasing silica nanoparticles Slomberg et al demonstrated that nanoparticles with decreased size and increased aspect ratio are more efficient against *S. aureus* and

P. aeruginosa biofilms than those with the bigger size. Simultaneously, improved anti-biofilm activity was noted for rod-shaped nanoparticles than spherical ones.[44] In another study, Li et co-workers reported that neutral and anionic charged CdSe–ZnS core-shell NPs are not able to efficiently penetrate biofilm and accumulate within its volume, while cationic particles are easily distributed, with the changes in the nanoparticles distribution being governed by their hydrophobicity.[45] Those reports highlight the importance of appropriate shaping of nanomaterials to obtain the optimal spectrum of physicochemical features and thus, appropriate killing efficiency and biofilm matrix disrupting ability. We believe that gold nanopeanuts exert suitable morphological features for efficient biofilm killing (Figure 1) – they have increased surface to volume ratio, when compared to spherical nanoparticles, but are also smaller (60 ± 5 nm along the longitudinal axis) than star-shaped gold nanoparticles, which core reaches even 243 nm at the farthest ends of the stars' arms.[18,21,46] We suggest that decreased activity of AuS NPs, when compared to other types of nanoparticles, is determined by the size of these structures and their limited ability to penetrate and be distributed evenly in the biofilm matrix. We believe it is also reasonable to consider that for the same reason AuS NPs are more affected by the presence of biofilm-promoting compounds than AuP NPs and AuSph (70C) NPs. It should be also noted, that peanut-shaped gold nanoparticles are characterized by the highest zeta potential in ions-enriched buffers, when compared to AuS NPs and AuSph (70C) NPs, which is why we believe that appropriate surface chemistry is a second factor contributing to the more efficient activity of gold nanopeanuts.

Extracellular DNA, high salt content, and magnesium ions are compounds present in excessive amounts in CF sputum and they can promote both bacterial infections and microbial biofilm development. Due to the polyanionic nature of extracellular DNA, a spectrum of positively-charged compounds, including cationic endogenous antimicrobial peptides, aminoglycosides, or positively-charged nanoparticles, is bound by eDNA, leading to resistance to applied treatment.[47–49] Particularly, gold itself exerts considerable affinity to DNA due to favorable Au-S chemistry.[50] According to our results, the presence of DNA results in some decrease of anti-biofilm abilities of nanoparticles, which do not rule out the possibility that some amount of AuNPs bind to DNA due to electrostatic attraction and covalent bonds formation (Figure 5). However, since nanoparticles are characterized by comparable surface chemistry and still are differently affected in DNA-containing growth media, we believe that observed effect is mostly size-dependent and AuP NPs and AuSph (70C) NPs, as the smaller ones, are potentially able to resist the effects of DNA associated with an increase of viscosity and limited access to biofilm-embedded bacteria. At the same time, we noted the decrease of the effectiveness of tobramycin (data not shown), which is in agreement with other reports demonstrating impairment of the bactericidal activity of aminoglycosides in CF sputum due to binding of those antibiotics to DNA.[51] At this aspect, maintaining the anti-biofilm activities of peanut-shaped gold nanoparticles is a favorable event with a great potential to be employed as a therapeutic agent in CF subjects, both alone or when combined with other antibiotics. Surprisingly, gold nanopeanuts were more affected by the increased sodium chloride content than DNA. Nevertheless, it should be noted that despite some decrease in anti-biofilm activity, gold nanopeanuts maintain satisfactory therapeutic efficiency in the ions-enriched environment (Figure 5).

Another approach to modifying the activity of nanoparticles is to combine them with EPS-targeting agents and thus, improve the accessibility of nanomaterials to bacterial cells. The utility of biofilm matrix-interacting agents was previously successfully tested for such drugs as Pulmozyme,[52] which encourages our studies. Our data demonstrate that in *Pseudomonas* biofilms, interfering with an extracellular matrix is beneficial for the improvement of the antimicrobial effect of nanoparticles. In this study, we used NAC as a mucolytic agent with a clinically-recognized effect on sputum viscosity and the ability to target EPS-compounds in biofilm, acting via breaking disulfide bridges between macromolecules.[53] In microbial biofilms, including those formed by *Pseudomonas*, disulfide bonds are the prerequisite for the stability of the extracellular substances. For instance, a crucial role of disulfide bonds was presented for (i) stability of FapC protein, an amyloid protein abundant in *P. aeruginosa* EPS,[54] (ii) maintaining the active conformation of extracellular lipases[55] or (iii) full proteolytic activity and structural stability of *Pseudomonas*-produced elastase.[56] We demonstrated that co-treatment of CF biofilms with NAC and peanut-shaped nanoparticles significantly improves anti-biofilm efficiency of AuP NPs (Figure 6), most likely by the improvement of nanoparticles diffusion and accessibility of nanoparticles to biofilm-embedded bacteria. This assumption is supported by a compelling number of previous reports revealing the possibility to improve nanoparticles penetration by adjuvant mucolytic therapies.[15,16] What is interesting, NAC-assisted facilitating of nanoparticles penetration is not enough if nanoparticles themselves do not possess favorable morphology and surface chemistry parameters.[16] Nevertheless, no similar research aiming to elucidate NAC-supported nanoparticles diffusion in bacterial biofilms was performed, which opens the opportunity to thoroughly investigate this phenomenon in more complex experimental settings. Naturally, we cannot exclude the possibility that improved effectiveness

of AuP NPs/NAC co-treatment does not result from the simple synergistic interactions between these compounds, since NAC possesses a well-recognized ability to affect growth, EPS production, and thus, biofilm formation by bacteria cells.[13] Nevertheless, our data collected during creep-recover experiments (Figure 7) demonstrated that NAC strongly affects rheological features of *Pseudomonas* biofilm, strongly suggesting that decreasing the biofilm viscosity is also a key factor contributing to upgraded AuP NPs effectiveness. Importantly, we also observed that the viscosity and recovery ability of biofilm is also affected by nanoparticles themselves (Figure 7). To date, there is little data about the impact of nanoparticles on biomaterials rheological properties and they are contradictory with each other. In 2010, Chen et al revealed that positively charged NPs can significantly reduce the rate of mucin matrix swelling and dispersion by forming NPs-mucin gel complexes, leading to decreasing the diffusivity and increasing the viscosity of mucin network. Such interaction might possibly affect the mucociliary transport.[57] On the other hand, according to the same research team, negatively-charged nanoparticles disperse mucin gels by enhancing network hydration, presenting the possibility to use carboxyl-functionalized NPs as mucus dispersant or mucolytic agent.[58] Reducing the viscosity and viscoelasticity of mucus, resulting from disruption of mucin-dominated meshwork was also reported for iron oxide Fe_2O_3 nanoparticles.[59] In our study, we present that peanut-shaped gold nanoparticles decrease the viscosity of the treated biofilms. Surprising is the fact, that while gold nanopeanuts fluidize the *Pseudomonas* biofilms, it is not sufficient to eradicate the formed biofilm and additional NAC co-treatment is required. We believe that this may be related to the fact that nanoparticles, due to their natural attraction to sulfur in disulfide bonds, exhibit the same mode of action as N-acetyl-cysteine and disturb the structure and stability of macromolecules that build the extracellular matrix of the biofilm. Potentially, nanoparticles trapped in the biofilm matrix have a greater affinity for disulfide bonds than for the bacterial membrane, and before they reach the level of a single cell, a significant pool of them will be used for interactions with the biofilm matrix. With the same mechanism, we also explain the fact that although an additive effect of NAC and AuP NPs is recorded, improvement of rheological parameters is not as prominent as we expected. We believe that due to strong mucolytic activity of NAC, the potential for further structural damage is already disproportionately lower, and the decrease in biofilm viscosity reached its maximum value for these experimental conditions. Based on above data, we believe that employment of peanut-shaped nanoparticles together with NAC might be useful for combined treatment of lung infections with the residual thick secretion of the bronchial tree. In this study, we present the potential utility of this approach in CF subject therapy, however we suggest to consider this option also in the treatment of medical conditions, in which NAC has a greater clinical value, such as chronic bronchitis or chronic obstructive pulmonary disease.[60] At the same time, some caution should be exercised with regard to the toxicity of nanoparticles, bearing in mind their potential interaction with disulfide bridges, which not only stabilize the structure of the biofilm, but above all, allow the maintenance of the correct structure of proteins and cellular macromolecules. Therefore, further research on the safety of such approach is desirable and should be continued.

An important observation noted in this study is the fact that the changes in viscosity parameters, supported by the inherent bactericidal activity of AuP NPs, augment the effect of tobramycin and allow the eradication of even drug-resistant pathogens. Due to a limited number of new antimicrobials effective for the treatment of CF lung infections, multi-compound therapy is becoming increasingly important in clinical practice and a spectrum of antibiotics is combined with other antimicrobials or nanoparticles themselves to identify those with the greatest antipseudomonal efficiency.[61–65] Our data reveal the possibility to combine non-spherical gold nanoparticles with conventional antibiotics against CF-derived bacterial biofilms, which we believe point out the possibility to develop novel therapeutic strategies.

Conclusion

In summary, we present that peanut-shaped gold nanoparticles should be considered as powerful therapeutic agents with the potential to be administrated simultaneously with antibiotics or mucolytics for efficient eradication of CF *Pseudomonas* biofilms. The strategy of biofilm EPS targeting, implemented by NAC and AuP NPs' biofilm viscosity-altering capabilities, was presented as sufficient to overcome antibiotic resistance of biofilms, including those formed by multidrug-resistant bacteria. Future work should focus on reducing the toxicity of the nanomaterials to mammalian cells. Moreover, the combination of AuP NPs with other therapeutic agents, including antibiotics, mucolytics, and anti-inflammatory drugs, should be further explored, as biofilm dispersal by peanut-shaped gold nanoparticles is likely to make the action of conventional therapeutics more effective.

Abbreviations

ACTs, airway clearance techniques; Au NPs, gold nanoparticles; AuP NPs, peanut-shaped gold nanoparticles; AuS NPs, star-shaped gold nanoparticles; AuSph (70C) NPs, porous, spherical-like gold nanoparticles synthetized using elevated temperatures; *C. albicans, Candida albicans*; CTAB, cetrimonium bromide; CF, cystic fibrosis; COS isolates, colistin-only-sensitive isolates; eDNA, extracellular DNA; EC50%, effective concentration at 50% level of population; EDS, energy-dispersive X-ray spectroscopy; EPS, extracellular polymeric substances; FT-Raman, Fourier Transform Raman spectroscopy; LB medium, Luria-Bertani medium; MIC, minimal inhibitory concentration; NAC, N-acetyl-cysteine; NaCl, natrium chloride; Mg^{2+}, magnesium ions; OD, optical density; *P. aeruginosa, Pseudomonas aeruginosa*; ROS, reactive oxygen species; *S. aureus, Staphylococcus aureus*; STEM, scanning transmission electron microscopy; XDR isolates, extensively drug-resistant isolates; ZP, zeta potential.

Ethics Approval

P. aeruginosa strains were isolated from the sputum of cystic fibrosis patients attending the Adult Cystic Fibrosis Center, University of Pennsylvania Health System, USA. Sputum samples and bacterial isolates were collected under approval of The University of Pennsylvania's Institutional Review Board (IRB) (no. 803255) and written informed consent was obtained from each patient.

Funding

This work was financially supported by grants from the National Science Centre, Poland: UMO-2018/30/M/NZ6/00502 (RB) and Medical University of Bialystok: SUB/1/DN/21/006/1122 (EP). Part of the study was conducted with the use of equipment purchased by the Medical University of Białystok as part of the RPOWP 2007-2013 funding, Priority I, Axis 1.1, contract No. UDA564 RPPD.01.01.00-20-001/15-00 dated 26.06.2015. The funders had no role in study design, data collection and analysis, decision to publish, or preparation of the manuscript.

Disclosure

JD and MP-W have a patent pending for synthesis and anti-cancer activity of gold nanopeanuts. The authors report no other conflicts of interest for this work.

References

1. Sawicki GS, Signorovitch JE, Zhang J, et al. Reduced mortality in cystic fibrosis patients treated with tobramycin inhalation solution. *Pediatr Pulmonol*. 2012;47(1):44–52. doi:10.1002/ppul.21521
2. Montero MM, López Montesinos I, Knobel H, et al. Risk Factors for Mortality among Patients with. *J Clin Med*. 2020;9(2):847. doi:10.3390/jcm9020514
3. Okamoto K, Gotoh N, Nishino T. Pseudomonas aeruginosa reveals high intrinsic resistance to penem antibiotics: penem resistance mechanisms and their interplay. *Antimicrob Agents Chemother*. 2001;45(7):1964–1971. doi:10.1128/AAC.45.7.1964-1971.2001
4. Høiby N, Ciofu O, Bjarnsholt T. Pseudomonas aeruginosa biofilms in cystic fibrosis. *Future Microbiol*. 2010;5(11):1663–1674. doi:10.2217/fmb.10.125
5. Bucki R, Niemirowicz K, Wnorowska U, et al. Polyelectrolyte-mediated increase of biofilm mass formation. *BMC Microbiol*. 2015;15:117. doi:10.1186/s12866-015-0457-x
6. Hurt K, Bilton D. Inhaled interventions in cystic fibrosis: mucoactive and antibiotic therapies. *Respiration*. 2014;88(6):441–448. doi:10.1159/000369533
7. Bucki R, Durnaś B, Wątek M, et al. Targeting polyelectrolyte networks in purulent body fluids to modulate bactericidal properties of some antibiotics. *Infect Drug Resist*. 2018;11:77–86. doi:10.2147/IDR.S145337
8. Karygianni L, Ren Z, Koo H, Thurnheer T. Biofilm Matrixome: extracellular Components in Structured Microbial Communities. *Trends Microbiol*. 2020;28(8):668–681. doi:10.1016/j.tim.2020.03.016
9. Tseng BS, Zhang W, Harrison JJ, et al. The extracellular matrix protects Pseudomonas aeruginosa biofilms by limiting the penetration of tobramycin. *Environ Microbiol*. 2013;15(10):2865–2878. doi:10.1111/1462-2920.12155
10. Peterson BW, He Y, Ren Y, et al. Viscoelasticity of biofilms and their recalcitrance to mechanical and chemical challenges. *FEMS Microbiol Rev*. 2015;39(2):234–245. doi:10.1093/femsre/fuu008
11. Zhao T, Liu Y. N-acetylcysteine inhibit biofilms produced by Pseudomonas aeruginosa. *BMC Microbiol*. 2010;10:140. doi:10.1186/1471-2180-10-140
12. Eroshenko D, Polyudova T, Korobov V. N-acetylcysteine inhibits growth, adhesion and biofilm formation of Gram-positive skin pathogens. *Microb Pathog*. 2017;105:145–152. doi:10.1016/j.micpath.2017.02.030

13. Olofsson AC, Hermansson M, Elwing H. N-acetyl-L-cysteine affects growth, extracellular polysaccharide production, and bacterial biofilm formation on solid surfaces. *Appl Environ Microbiol*. 2003;69(8):4814–4822. doi:10.1128/AEM.69.8.4814-4822.2003
14. Leite B, Gomes F, Teixeira P, Souza C, Pizzolitto E, Oliveira R. Combined effect of linezolid and N-acetylcysteine against Staphylococcus epidermidis biofilms. *Enferm Infecc Microbiol Clin*. 2013;31(10):655–659. doi:10.1016/j.eimc.2012.11.011
15. Suk JS, Boylan NJ, Trehan K, et al. N-acetylcysteine enhances cystic fibrosis sputum penetration and airway gene transfer by highly compacted DNA nanoparticles. *Mol Ther*. 2011;19(11):1981–1989. doi:10.1038/mt.2011.160
16. Suk JS, Lai SK, Boylan NJ, Dawson MR, Boyle MP, Hanes J. Rapid transport of muco-inert nanoparticles in cystic fibrosis sputum treated with N-acetyl cysteine. *Nanomedicine*. 2011;6(2):365–375. doi:10.2217/nnm.10.123
17. Blasi F, Page C, Rossolini GM, et al. The effect of N-acetylcysteine on biofilms: implications for the treatment of respiratory tract infections. *Respir Med*. 2016;117:190–197. doi:10.1016/j.rmed.2016.06.015
18. Piktel E, Suprewicz T, Depciuch J, et al. Varied-shaped gold nanoparticles with nanogram killing efficiency as potential antimicrobial surface coatings for the medical devices. *Sci Rep*. 2021;11(1):12546. doi:10.1038/s41598-021-91847-3
19. Piktel E, Suprewicz L, Depciuch J, et al. Rod-shaped gold nanoparticles exert potent candidacidal activity and decrease the adhesion of fungal cells. *Nanomedicine*. 2020;15(28):2733–2752. doi:10.2217/nnm-2020-0324
20. Cabuzu D, Cirja A, Puiu R, Grumezescu AM. Biomedical applications of gold nanoparticles. *Curr Top Med Chem*. 2015;15(16):1605–1613. doi:10.2174/1568026615666150414144750
21. Chmielewska SJ, Skłodowski K, Depciuch J, et al. Bactericidal Properties of Rod-, Peanut-, and Star-Shaped Gold Nanoparticles Coated with Ceragenin CSA-131 against Multidrug-Resistant Bacterial Strains. *Pharmaceutics*. 2021;13(3):425. doi:10.3390/pharmaceutics13030425
22. Trejo-Hernández A, Andrade-Domínguez A, Hernández M, Encarnación S. Interspecies competition triggers virulence and mutability in Candida albicans-Pseudomonas aeruginosa mixed biofilms. *ISME J*. 2014;8(10):1974–1988. doi:10.1038/ismej.2014.53
23. Garg N, Scholl C, Mohanty A, Jin R. The role of bromide ions in seeding growth of Au nanorods. *Langmuir*. 2010;26(12):10271–10276. doi:10.1021/la100446q
24. Grzelczak M, Pérez-Juste J, Mulvaney P, Liz-Marzán LM. Shape control in gold nanoparticle synthesis. *Chem Soc Rev*. 2008;37(9):1783–1791. doi:10.1039/b711490g
25. Jana NR, Gearheart L, Murphy CJ. Seed-Mediated Growth Approach for Shape-Controlled Synthesis of Spheroidal and Rod-like Gold Nanoparticles Using a Surfactant Template. *Advances Materials*. 2001;13(18):1389–1393. doi:10.1002/1521-4095(200109)13:18<1389::AID-ADMA1389>3.0.CO;2-F
26. Nikoobakht B, El-Sayed MA. Preparation and Growth Mechanism of Gold Nanorods (NRs) Using Seed-Mediated Growth Method. *Chemistry of Materials*. 2003;15(10):1957–1962. doi:10.1021/cm020732l
27. Depciuch J, Stec M, Kandler M, Baran J, Parlinska-Wojtan M. From spherical to bone-shaped gold nanoparticles-Time factor in the formation of Au NPs, their optical and photothermal properties. *Photodiagnosis Photodyn Ther*. 2020;30:101670. doi:10.1016/j.pdpdt.2020.101670
28. Wnorowska U, Piktel E, Durnaś B, Fiedoruk K, Savage PB, Bucki R. Use of ceragenins as a potential treatment for urinary tract infections. *BMC Infect Dis*. 2019;19(1):369. doi:10.1186/s12879-019-3994-3
29. Piktel E, Pogoda K, Roman M, et al. Sporicidal activity of ceragenin CSA-13 against Bacillus subtilis. *Sci Rep*. 2017;7:44452. doi:10.1038/srep44452
30. Magiorakos AP, Srinivasan A, Carey RB, et al. Multidrug-resistant, extensively drug-resistant and pandrug-resistant bacteria: an international expert proposal for interim standard definitions for acquired resistance. *Clin Microbiol Infect*. 2012;18(3):268–281. doi:10.1111/j.1469-0691.2011.03570.x
31. Bos AC, Passé KM, Mouton JW, Janssens HM, Tiddens HA. The fate of inhaled antibiotics after deposition in cystic fibrosis: how to get drug to the bug? *J Cyst Fibros*. 2017;16(1):13–23. doi:10.1016/j.jcf.2016.10.001
32. Shigeta M, Tanaka G, Komatsuzawa H, Sugai M, Suginaka H, Usui T. Permeation of antimicrobial agents through Pseudomonas aeruginosa biofilms: a simple method. *Chemotherapy*. 1997;43(5):340–345. doi:10.1159/000239587
33. Walters MC, Roe F, Bugnicourt A, Franklin MJ, Stewart PS. Contributions of antibiotic penetration, oxygen limitation, and low metabolic activity to tolerance of Pseudomonas aeruginosa biofilms to ciprofloxacin and tobramycin. *Antimicrob Agents Chemother*. 2003;47(1):317–323. doi:10.1128/aac.47.1.317-323.2003
34. Pai VB, Nahata MC. Efficacy and safety of aerosolized tobramycin in cystic fibrosis. *Pediatr Pulmonol*. 2001;32(4):314–327. doi:10.1002/ppul.1125
35. Moreau-Marquis S, Stanton BA, O'Toole GA. Pseudomonas aeruginosa biofilm formation in the cystic fibrosis airway. *Pulm Pharmacol Ther*. 2008;21(4):595–599. doi:10.1016/j.pupt.2007.12.001
36. Sherrard LJ, Tunney MM, Elborn JS. Antimicrobial resistance in the respiratory microbiota of people with cystic fibrosis. *Lancet*. 2014;384(9944):703–713. doi:10.1016/S0140-6736(14)61137-5
37. Nasser F, Davis A, Valsami-Jones E, Lynch I. Shape and Charge of Gold Nanomaterials Influence Survivorship, Oxidative Stress and Moulting of Daphnia magna. *Nanomaterials*. 2016;6(12):222. doi:10.3390/nano6120222
38. Bhatia E, Banerjee R. Hybrid silver-gold nanoparticles suppress drug resistant polymicrobial biofilm formation and intracellular infection. *J Mater Chem B*. 2020;8(22):4890–4898. doi:10.1039/d0tb00158a
39. Li X, Robinson SM, Gupta A, et al. Functional gold nanoparticles as potent antimicrobial agents against multi-drug-resistant bacteria. *ACS Nano*. 2014;8(10):10682–10686. doi:10.1021/nn5042625
40. Elbehiry A, Al-Dubaib M, Marzouk E, Moussa I. Antibacterial effects and resistance induction of silver and gold nanoparticles against Staphylococcus aureus-induced mastitis and the potential toxicity in rats. *Microbiologyopen*. 2019;8(4):e00698. doi:10.1002/mbo3.698
41. Lee B, Lee DG. Synergistic antibacterial activity of gold nanoparticles caused by apoptosis-like death. *J Appl Microbiol*. 2019;127(3):701–712. doi:10.1111/jam.14357
42. Ruddaraju LK, Pammi SVN, Guntuku GS, Padavala VS, Kolapalli VRM. A review on anti-bacterials to combat resistance: from ancient era of plants and metals to present and future perspectives of green nano technological combinations. *Asian J Pharm Sci*. 2020;15(1):42–59. doi:10.1016/j.ajps.2019.03.002

43. Niemirowicz K, Piktel E, Wilczewska AZ, et al. Core-shell magnetic nanoparticles display synergistic antibacterial effects against Pseudomonas aeruginosa and Staphylococcus aureus when combined with cathelicidin LL-37 or selected ceragenins. *Int J Nanomedicine*. 2016;11:5443–5455. doi:10.2147/IJN.S113706
44. Slomberg DL, Lu Y, Broadnax AD, Hunter RA, Carpenter AW, Schoenfisch MH. Role of size and shape on biofilm eradication for nitric oxide-releasing silica nanoparticles. *ACS Appl Mater Interfaces*. 2013;5(19):9322–9329. doi:10.1021/am402618w
45. Li X, Yeh YC, Giri K, et al. Control of nanoparticle penetration into biofilms through surface design. *Chem Commun (Camb)*. 2015;51(2):282–285. doi:10.1039/c4cc07737g
46. Piktel E, Ościłowska I, Suprewicz Ł, et al. ROS-Mediated Apoptosis and Autophagy in Ovarian Cancer Cells Treated with Peanut-Shaped Gold Nanoparticles. *Int J Nanomedicine*. 2021;Volume 16:1993–2011. doi:10.2147/IJN.S277014
47. Mulcahy H, Charron-Mazenod L, Lewenza S. Extracellular DNA chelates cations and induces antibiotic resistance in Pseudomonas aeruginosa biofilms. *PLoS Pathog*. 2008;4(11):e1000213. doi:10.1371/journal.ppat.1000213
48. Hiebner DW, Barros C, Quinn L, Vitale S, Casey E. Surface functionalization-dependent localization and affinity of SiO. *Biofilm*. 2020;2:100029. doi:10.1016/j.bioflm.2020.100029
49. Wnorowska U, Watek M, Durnas B, et al. Extracellular DNA as an essential component and therapeutic target of microbial biofilm. *Medical Studies-Studia Medyczne*. 2015;31(2):132–138. doi:10.5114/ms.2015.52912
50. Carnerero JM, Jimenez-Ruiz A, Castillo PM, Prado-Gotor R. Covalent and Non-Covalent DNA-Gold-Nanoparticle Interactions: new Avenues of Research. *Chemphyschem*. 2017;18(1):17–33. doi:10.1002/cphc.201601077
51. Chiang WC, Nilsson M, Jensen P, et al. Extracellular DNA shields against aminoglycosides in Pseudomonas aeruginosa biofilms. *Antimicrob Agents Chemother*. 2013;57(5):2352–2361. doi:10.1128/AAC.00001-13
52. Hall-Stoodley L, Nistico L, Sambanthamoorthy K, et al. Characterization of biofilm matrix, degradation by DNase treatment and evidence of capsule downregulation in Streptococcus pneumoniae clinical isolates. *BMC Microbiol*. 2008;8:173. doi:10.1186/1471-2180-8-173
53. Wallis C. Mucolytic therapy in cystic fibrosis. *J R Soc Med*. 2001;94(Suppl 40):17–24. doi:10.1177/014107680109440s06
54. Bleem A, Christiansen G, Madsen DJ, et al. Protein Engineering Reveals Mechanisms of Functional Amyloid Formation in Pseudomonas aeruginosa Biofilms. *J Mol Biol*. 2018;430(20):3751–3763. doi:10.1016/j.jmb.2018.06.043
55. Liebeton K, Zacharias A, Jaeger KE. Disulfide bond in Pseudomonas aeruginosa lipase stabilizes the structure but is not required for interaction with its foldase. *J Bacteriol*. 2001;183(2):597–603. doi:10.1128/JB.183.2.597-603.2001
56. Braun P, Ockhuijsen C, Eppens E, Koster M, Bitter W, Tommassen J. Maturation of Pseudomonas aeruginosa elastase. Formation of the disulfide bonds. *J Biol Chem*. 2001;276(28):26030–26035. doi:10.1074/jbc.M007122200
57. Chen EY, Wang YC, Chen CS, Chin WC. Functionalized positive nanoparticles reduce mucin swelling and dispersion. *PLoS One*. 2010;5(11):e15434. doi:10.1371/journal.pone.0015434
58. Chen EY, Daley D, Wang YC, Garnica M, Chen CS, Chin WC. Functionalized carboxyl nanoparticles enhance mucus dispersion and hydration. *Sci Rep*. 2012;2:211. doi:10.1038/srep00211
59. Deng L, Luo M, Wang J, et al. Fe2O3 Nanoparticles Cause Alteration of Microstructure and Rheological Properties of Simulated Mucus. *Am J Respir Crit Care Med*. 2016;1:85.
60. Cazzola M, Calzetta L, Page C, et al. Influence of N-acetylcysteine on chronic bronchitis or COPD exacerbations: a meta-analysis. *Eur Respir Rev*. 2015;24(137):451–461. doi:10.1183/16000617.00002215
61. Kapoor P, Murphy P. Combination antibiotics against. *Heliyon*. 2018;4(3):e00562. doi:10.1016/j.heliyon.2018.e00562
62. Campana S, Taccetti G, Farina S, Ravenni N, de Martino M. Antimicrobial susceptibility and synergistic activity of meropenem against Gram-negative non-fermentative bacteria isolated from cystic fibrosis patients. *J Chemother*. 2003;15(6):551–554. doi:10.1179/joc.2003.15.6.551
63. Habash MB, Goodyear MC, Park AJ, et al. Potentiation of Tobramycin by Silver Nanoparticles against Pseudomonas aeruginosa Biofilms. *Antimicrob Agents Chemother*. 2017;61(11). doi:10.1128/AAC.00415-17
64. Habash MB, Park AJ, Vis EC, Harris RJ, Khursigara CM. Synergy of silver nanoparticles and aztreonam against Pseudomonas aeruginosa PAO1 biofilms. *Antimicrob Agents Chemother*. 2014;58(10):5818–5830. doi:10.1128/AAC.03170-14
65. Salman M, Rizwana R, Khan H, et al. Synergistic effect of silver nanoparticles and polymyxin B against biofilm produced by. *Artif Cells Nanomed Biotechnol*. 2019;47(1):2465–2472. doi:10.1080/21691401.2019.1626864

Infection and Drug Resistance Dovepress

Publish your work in this journal

Infection and Drug Resistance is an international, peer-reviewed open-access journal that focuses on the optimal treatment of infection (bacterial, fungal and viral) and the development and institution of preventive strategies to minimize the development and spread of resistance. The journal is specifically concerned with the epidemiology of antibiotic resistance and the mechanisms of resistance development and diffusion in both hospitals and the community. The manuscript management system is completely online and includes a very quick and fair peer-review system, which is all easy to use. Visit http://www.dovepress.com/testimonials.php to read real quotes from published authors.

Submit your manuscript here: https://www.dovepress.com/infection-and-drug-resistance-journal